IEEE Access
Multidisciplinary | Rapid Review | Open Access Journal

Received April 1, 2019, accepted April 15, 2019, date of publication April 22, 2019, date of current version April 30, 2019.

Digital Object Identifier 10.1109/ACCESS.2019.2912376

Power Quality Control of Smart Hybrid AC/DC Microgrids: An Overview

FARZAM NEJABATKHAH, (Member, IEEE), YUN WEI LI, (Senior Member, IEEE), AND HAO TIAN, (Student Member, IEEE)

Department of Electrical and Computer Engineering, University of Alberta, Edmonton, AB T6G 1H9, Canada

Corresponding author: Farzam Nejabatkhah (nejabatk@ualberta.ca)

ABSTRACT Today, conventional power systems are evolving to smart grids, which encompass clusters of AC/DC microgrids, interfaced through power electronics converters. In such systems, increasing penetration of the power electronics-based distributed generations, energy storages, and modern loads provide a great opportunity for power quality control. In this paper, an overview of the power quality control of smart hybrid AC/DC microgrids is presented. Different types of power quality issues are studied first, with consideration of real-world hybrid microgrid examples, including data centers, electric railway systems, and electric vehicles charging stations. It shows that compared to traditional centralized power quality compensations, smart interfacing power converters from distributed generations, energy storages, and loads, and the AC and DC subgrids interfacing converters are promising candidates for power quality control. To realize the smart interfacing converters' power quality control, both primary converters control and secondary system coordination are required. In this paper, a thorough review of the primary control of interfacing converters to integrate the power quality compensation are presented, with a focus on the hybrid AC/DC microgrid harmonics compensation and unbalance compensation. For multiple interfacing converters, the secondary control with system-level coordination and optimization for harmonics and unbalance compensation (considering both unbalance and harmonics in single-phase and three-phase systems) are also presented. Challenges like low switching frequency of interfacing converters, parallel interfacing converters operation, and interfacing converters communications are discussed, and typical solutions for primary and secondary controls to deal with them are presented. The paper also includes rich case study results.

INDEX TERMS Harmonic compensation, hybrid AC/DC microgrid, interfacing power electronics converters, power quality, primary and secondary control, smart converters, smart grids, unbalance compensation.

I. INTRODUCTION

Smart grids are emerging as next-generation of power systems, which contain interconnected clusters of microgrids. These microgrids encompass AC and DC subgrids, called hybrid microgrids. Such hybrid microgrids are power electronic-based autonomous systems in which most generations are distributed and usually from renewable resources [1]. As more power electronic converters from distributed generations, energy storage systems, loads etc. are used, new opportunities for power system control are emerging. Based on the Electric Power Research Institute (EPRI) and the Smart Electric Power Alliance (SEPA) reports, the smart power converters are introduced as a least-cost tool for supporting the grid and mitigating grid challenges [2]–[4]. The recent revisions of standards and grid codes (such as IEEE 1547 [5], and California's Rule 21 [6]), as well as communication protocols also encourage the use of smart power converters' functions. However, it should be considered that most of the converters are not utility-owned and operated resources. Thus, appropriate policies and markets are required to encourage more ancillary functions. For example, Arizona Public Service (APS) is working on the installation of smart power converters for about 1,500 home solar systems (about 10 megawatts in total). They devote $30 per month bill credit for participants for 20 years for turning over their inverters to real-time controls and utility data collection that can be used for ancillary services [2], [4].

In hybrid microgrids, increasing single-phase/unbalanced loads, non-linear loads, and single-phase/unbalance distributed generations leads to power quality challenges. For example, more efficient loads such as Compact Fluorescent

The associate editor coordinating the review of this manuscript and approving it for publication was Giambattista Gruosso.

Lamp (CFL), LED, adjustable speed drives (ASD) fridge, etc. produce high current harmonics in the residential distribution system, and it is expected that the residential system voltage THD reaches 5% soon in North America [7]. Although additional devices can be installed to address the power quality issues (for example, FACTS devices, filters, etc.), they increase total investment cost. Using the smart power converters for power quality management is a promising idea since most of them are not operating at full rating all the time due to the intermittent nature of renewable energy sources. Therefore, the available ratings of the converters can be smartly controlled to improve the power quality issues in addition to their power management targets.

In this paper, the smart hybrid AC/DC microgrids' power quality controls are reviewed. Different structures of the hybrid AC/DC microgrids are discussed first. Then, various power quality issues with consideration of real-world hybrid microgrid examples including data centers, electric railway systems, electric vehicles charging stations, and residential distribution systems are studied. In this paper, the smart interfacing converters (IFCs) from distributed generations, energy storages, loads, as well as the AC and DC subgrids interfacing converters are introduced as promising candidates for power quality control. The primary controls of interfacing power converters are thoroughly reviewed to integrate the power quality compensation capability, including harmonics compensation and unbalance compensation. Also, the secondary control with system-level coordination and optimization for harmonics and unbalance compensation in the single-phase and three-phase systems are studied. This paper also addresses some challenges of IFCs including low switching frequency, parallel operation, and communications, and the typical modifications for primary and secondary controls to deal with them are discussed. In this paper, comprehensive examples are provided to support the reviewed control strategies.

This paper is organized as follows. In Section II, structures of hybrid AC/DC microgrids and their power quality issues with real-world examples are provided. The interfacing converters' primary and secondary control strategies are addressed in Section III. In Section IV, unbalance compensation in hybrid AC/DC microgrids through smart interfacing converters is studied. The harmonic compensation in hybrid AC/DC microgrids by using interfacing converters is discussed in Section V. Finally, Section VI summarizes the discussions and lists conclusions and future trends.

II. HYBRID AC/DC MICROGRIDS AND POWER QUALITY ISSUES

A. STRUCTURES OF HYBRID AC/DC MICROGRIDS

In general, structures of hybrid microgrids can be classified into AC-coupled, DC-coupled, and AC-DC-coupled microgrids [8]. In the AC-coupled microgrids, various distributed generations (DGs), storage elements (SEs) and loads are connected to the common AC bus/subgrid. This is the dominant structure now due to the simple installation and control of DGs/SEs. Also, the AC voltage/frequency control of AC-coupled microgrid is easier than other hybrid microgrids' structures, where DC subgrids are interacted with the AC subgrids. In this structure, the high-frequency AC bus is possible. In the DC-coupled structure, DGs, SEs and loads are connected to the common DC bus/subgrid, and the AC-DC buses/subgrids are connected through the interfacing converters. The DC-coupled microgrid features simple structure and does not need any synchronization when integrating different DGs. As a most promising future microgrid structure, the AC-DC-coupled microgrids contain DGs and SEs in both AC and DC buses/subgrid. A typical example of the AC-DC-coupled hybrid AC/DC microgrid is shown in Fig. 1, which can be considered as a general form of the AC-coupled and DC-coupled hybrid microgrids. This structure requires more coordination between the DC and AC subgrids. More information about the hybrid microgrid structures and their control schemes can be found in [8].

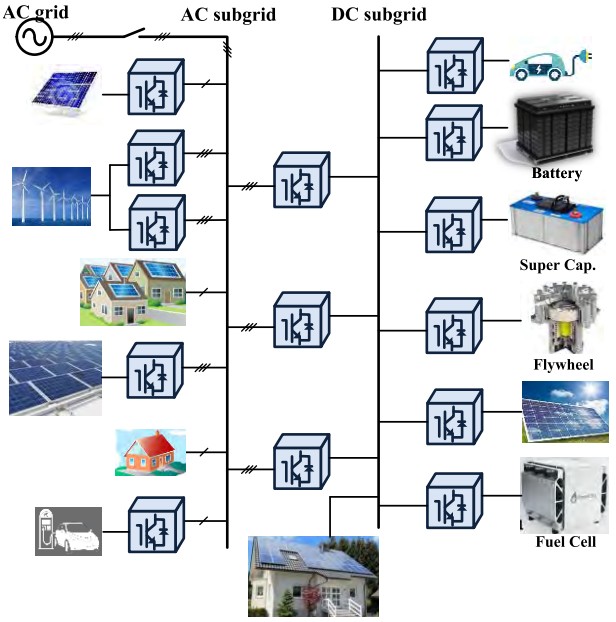

FIGURE 1. A typical structure of AC-DC-coupled hybrid microgrid.

As a few examples of grid-connected hybrid microgrids, data centers, electric vehicles (EVs) charging stations, and electric railway systems can be named. The structures of data centers are usually AC-coupled; however, research and implementation of the DC data centers have been already started (they have better performance compare to AC architecture in terms of reliability, efficiency, and power quality) [9]–[12]. The EVs charging stations have AC and DC structures [13]–[18]. However, due to the DC voltage required for charging EVs batteries, easier renewable energy integrations, and higher efficiency and better power quality, DC structure is more promising. The electric railway system is another example of the hybrid microgrid that has DC and AC structures [19]–[21].

B. POWER QUALITY ISSUES IN HYBRID MICROGRIDS

The power quality issues are becoming urgent for future hybrid microgrids due to increasing penetration of single-phase/unbalance loads, non-linear loads, and single-phase/unbalance distributed generations. In general, the power quality issues in the DC subgrid can be voltage variations and harmonics. In the AC subgrid, voltage variations, unbalances, and harmonics are major power quality concerns.

To improve such power quality issues, additional compensation devices can be installed. For example, the AC-side three-phase unbalance condition can be compensated by installing power electronics-based equipment such as a unified power quality conditioner (UPQC), static synchronous compensators (STATCOM), etc. As another example, the harmonics in the AC subgrid can be mitigated by using passive power filters (PPFs) and active power filters (APFs), and the DC-side harmonics and variations can be easily filtered by installed large capacitors and tuned filters. In following, a few examples of the power quality issues in the real-world hybrid microgrids are discussed, and the compensation techniques are provided.

Data Center: Based on EPRI report, data centers will consume 20% electricity in the United States by 2030, and power quality issues are very important concern in such systems (in the United States, poor power quality and unreliable power supply of data centers can result in millions of dollar loss annually) [22]. In the AC data centers, voltage sags and momentary interruptions, as well as harmonics, are the power quality issues [22]–[24]. Since the availability of the data centers is critical, UPS and backup generator are used to deal with voltage sags and momentary interruptions [22]. However, the main power quality concern is harmonics [22]–[24], which are produced by UPSs, power converters (e.g. rectifiers), variable speed drives, fluorescent lights, transformer inrush current, battery chargers, non-PFC electronic loads, etc. in data centers. As an example, the measured current harmonics at the grid-connected point in the Libyan Telecom Technology (LTT) headquarter and data center showed the presence of low-order current harmonics including 3^{rd}, 5^{th}, 7^{th}, and 9^{th} with the values of 7%, 16%, 11%, and 3% of the fundamental current [25]. The harmonics in AC data centers can be compensated using filters (active, passive, series/parallel resonant filter, etc.) and power conditioners [22]–[24]. In DC data centers, voltage ripples and harmonics are power quality issues, caused by AC system unbalance voltage or/and DC side components. The power quality issues have not been studied in detail for DC data centers yet.

Electric Vehicles (EVs) Charging Stations: The power quality issues in charging stations are voltage fluctuations, harmonics, and unbalances as well as current harmonics (main issue for now). As an example, the monthly measured total harmonic distortion (THD) of voltage in the EV charging station in Taiwan showed that the THD is higher than 1.5% in some days [26]. In general, the power quality issues mainly depend on the structure of stations. For example, in the onboard charger, where power factor correction (PFC) and pulse width modulation (PWM) control techniques are used, the generated harmonics are small [26]. However, in the presence of 12-pulse diode rectifier in DC stations, low order harmonics are produced [27]. The power quality issues in the EV charging stations can be compensated by using active power filters, PWM rectifiers, and power factor correction (PFC) stages [28]–[34]. It should be mentioned that the power quality control in the EVs' charging station is quite new topics and more study should be done in this field.

*Electric Railway Systems:*The common power quality issues in the railway systems are three-phase unbalance voltage (AC railway systems are usually single-phase), voltage fluctuation, resonance (PWM control of converters may create resonance with railway power systems), and harmonics [19]–[21], [35], [36]. In practice, to solve the power quality issues in the railway systems, FACTS devices are installed [21], [37]–[40]. For example, ABB has a demonstration AC railway system that the STATCOM can reduce its unbalanced voltage from 3% to 1% [21].

Residential distribution system: Although the three-phase unbalance voltage due to the presence of single-phase/unbalance loads and distributed generations is an important power quality concern, the current harmonics in such systems are also increasing rapidly. In detail, increasing more-efficient loads such as CFL, LED, ASD fridge, high-efficiency washer, etc. in residential distribution microgrids produce high harmonics due to their non-linear characteristics [7]. For example, the CFL produces 3^{rd}, 5^{th}, and 7^{th}-order current harmonics with the value of 87%, 60%, and 47% of the fundamental harmonic, and the values of those harmonics in LED are 73%, 26%, and 27% of the fundamental current [7]. In the residential distribution system, FACTS devices and filters are commonly installed for the unbalanced voltage and harmonics compensations.

Considering the aforementioned discussions, the traditional centralized compensation methods can be used to mitigate power quality issues. However, installing additional equipment increases the total investment cost. Also, the centralized power quality compensation does not work well since sources of power quality issues are widely distributed in the microgrids. Due to increasing penetration of smart interfacing converters (IFCs) from distributed generations (DGs), storage elements (SEs), loads, and DC-AC subgrids interfacing converters in the hybrid AC/DC microgrids, they can be great candidates to help address the power quality issues in addition to their power management targets. This idea is promising since most of them are not operating at their full rating all the time due to renewable energy intermittent nature. So, available ratings are used to improve the power quality issues. In this paper, important power quality issues in the hybrid AC/DC microgrids including harmonics in DC side and unbalance condition and harmonics in the AC side as well as their interactions are discussed in detail.

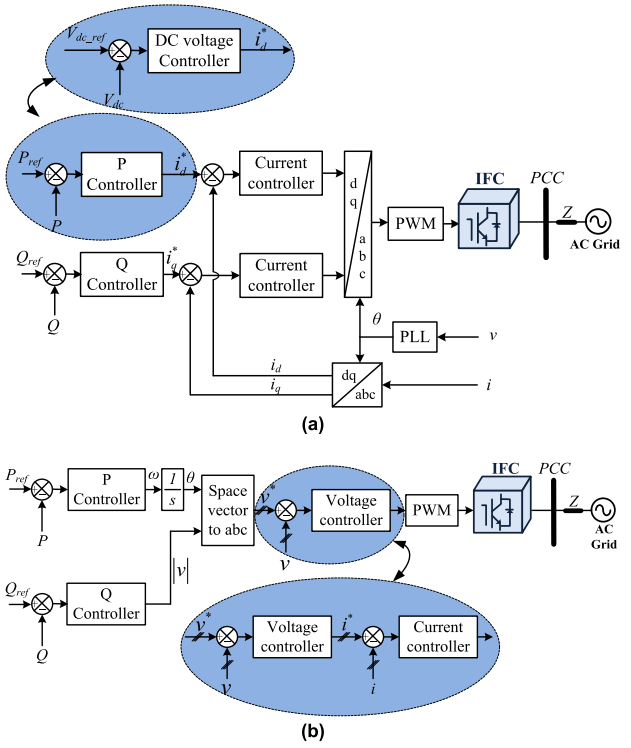

FIGURE 2. Primary control of IFCs; a) bi-directional power control through current control method (CCM), b) bi-directional power control through voltage control method (VCM).

III. INTERFACING CONVERTERS CONTROL

A. PRIMARY CONTROL OF INTERFACING CONVERTERS

In general, the interfacing converter's bi-directional power control can be realized either by the current control method (CCM) or voltage control method (VCM) [41], [42]. In Fig. 2(a), the DC-AC IFC control with CCM is shown. As seen from the figure, in the CCM, the d-axis and q-axis reference currents are produced by active and reactive power controllers, respectively. It should be noted that the active and reactive powers references can be achieved from outer supervisory control layer (e.g. power management scheme). Also, the d-axis reference current can be generated by dc-link voltage control, especially in two-stage interfacing converters (DC-DC and DC-AC converters where active power is controlled by DC-DC converter). In general, the CCM-based IFC control is mainly used in the grid-connected operation mode where the AC bus frequency and voltage are determined by other power sources or the gird.

In the VCM-based control strategy, the output voltage of IFC is controlled to regulate the output active and reactive powers (IFC behaves like a synchronous generator). The VCM control strategy is shown in Fig. 2(b). Considering that the linking impedance of IFC is mainly inductive (in VCM, a linking impedance (physical or virtual) is necessary between the converter and grid) and the phase angle between IFC voltage and the AC bus voltage vectors are typically small, the active power flow of IFC is controlled by the AC voltage frequency and the reactive power flow is controlled by the AC voltage magnitude. This control strategy can be used in both grid-connected and islanded modes. The active and reactive power controllers are usually proportional controllers (k_p and k_q) for realizing P-f and Q-V droop control [43], [44]. The more complex controller can also be used here to closely mimic the dynamics of a synchronous generator with excitation and torque [45], [46].

It should be highlighted that with the generated reference current/voltage from the two control methods in Fig. 2, the IFC output current/voltage can then be controlled in the synchronous dq frame or in the stationary $\alpha\beta$ frame (e.g. here CCM-based IFC controller is in synchronous dq frame).

B. SUPERVISORY CONTROL OF INTERFACING CONVERTERS

In the smart hybrid microgrids, the interfacing converters are communicated with supervisory control center (SCC). The SCC receives data from the IFCs and from power system measurement devices and makes decisions based on defined objectives. Then, the decision signals are sent to all the IFCs local controllers (where the primary control of IFCs are running). In general, the supervisory control can be separated into secondary and tertiary controls [47]. The objectives of secondary control include system frequency restoration, unbalanced voltage compensation, harmonic compensation, etc. The tertiary control is usually used to determine the operating point of each power sources (real and reactive powers), and usually, the optimization problem is run to achieve a global optimum. The structures of the supervisory control of IFCs can be categorized as centralized, distributed, and master-slave, which are presented in Fig. 3. In a centralized structure, all the IFCs communicate with one SCC, and the central SCC makes decisions based on the objectives and constraints. Since all system data are gathered in one center, the global optimal operating point can be achieved. However, heavy computation burden and communication failure possibility (may cause overall shut down in the system) are challenges of this structure. In distributed structure, groups of IFCs communicate with their SCCs, and the SCCs communicate with each other. This structure is useful for clustered interconnected microgrids and multi-agent control strategies. In the distributed structure, the computation burden of each SCC is reduced, and the redundancy and modularity of the system are increased. Also, failure in the communication link will not affect the entire system. The master-slave structure is popular for the IFCs close to each other, where the local controller of one of IFCs acts as the SCC. In this structure, all the IFCs communicate with each other. It should be mentioned that in some cases the primary and supervisory controllers are run in the local controllers of interfacing converters (e.g. individual three-phase IFCs control for unbalanced condition compensation, which will be discussed later). Various examples of supervisory control of IFCs will be provided in Section IV and Section V.

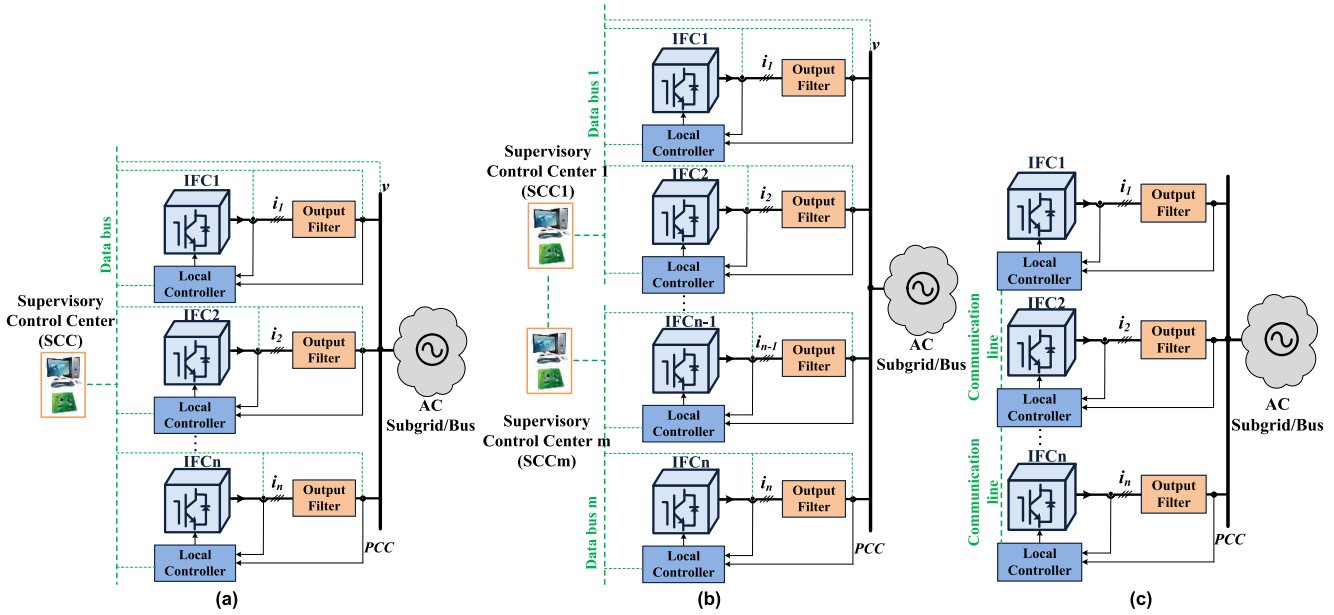

FIGURE 3. Structures of supervisory control of IFCs; a) centralized structure, b) distributed structure and c) master-slave structure.

IV. UNBALANCE COMPENSATION IN HYBRID AC/DC MICROGRIDS THROUGH SMART INTERFACING CONVERTERS

In general, the unbalance condition is caused by the ever-increasing unbalanced distribution of single-phase/unbalanced loads, single-phase/unbalanced distributed generations, and remote grid faults. Based on American National Standards Institute (ANSI) and IEEE standard, the unbalanced voltage level should be less than 3%, and it should be less than 2% in the International Electrotechnical Commission (IEC) standard [36], [48], [49].

The unbalanced voltage has adverse effects on the power system and equipment including electrical machine overheating, transformer overloading, capacity limitation of power electronics devices, more losses and less stability of power system, negative impacts on induction motors and adjustable speed drives [36], [50], [51]. In addition, the unbalanced voltage introduces adverse effects on the power electronic interfacing converters. The peak current increase in the same power production of IFC and double-frequency power oscillations at the output of three-phase power converters, which are reflected as a ripple in the DC link voltage, are the adverse effects of the unbalance voltage on IFCs' operation. These adverse effects may lead to instability or system protection if the DC bus voltage exceeds the maximum limit, affect DC converters and loads in the DC subgrid, and may result in over-current protection.

In general, the unbalanced voltage can be compensated using power electronics-based equipment including series active power filter by injecting negative sequence voltage [52], [53], shunt active power filter by injecting negative sequence current [54], [55], series-parallel compensators such as unified power quality conditioner (UPQC) by injecting negative sequence voltage with series converter and negative sequence current with parallel converter [56], and static synchronous compensators (STATCOM) by injecting positive and negative sequence reactive powers [50], [57], [58]. Moreover, passive devices such as shunt capacitor can also be used for unbalanced voltage compensation [59], [60].

However, as mentioned, the power electronics interfacing converters in the hybrid AC/DC microgrids can provide better unbalance compensation in terms of cost and effectiveness. Such interfacing converters can be three-phase and single-phase converters. In following, control strategies of the IFCs under unbalance voltage are reviewed in detail.

A. CONTROL OF INDIVIDUAL THREE-PHASE IFCS UNDER UNBALANCE VOLTAGE

The three-phase IFCs are used to connect DGs/SEs to the AC subgrid as well as to interlink DC and AC subgrids. The individual three-phase IFCs has two main control options under unbalance condition:

- **Active compensation of the PCC unbalanced voltage:** In this control strategy, the level of unbalance compensation can be controlled directly, while the adverse effects may or may not be controlled. Thus, this control method can be classified as:
  Adjustable compensation *of unbalanced voltage and adverse effects control:* The IFC's output active power oscillation and/or its peak current are controlled directly as well. In [61]–[63], the unbalanced voltage compensation has been considered together with IFC peak current control while IFC output active power oscillation control has been considered in [64]. In [65], both the active power oscillation and peak current control in

addition to adjustable unbalance compensation has been addressed.

Adjustable compensation of unbalanced voltage without direct control of adverse effects: The IFC's output active power oscillation and/or its peak current are not controlled directly, which can provide more reduction of unbalance condition. In [65]–[69], the adjustable unbalance compensation without adverse effects consideration is discussed. For example, in [65], the minimization of the PCC unbalanced voltage is addressed without IFC's power oscillation consideration.

- **Control of unbalance voltage adverse effects on IFC operation:** In this control strategy, the PCC unbalanced voltage compensation level is not controlled directly. This control strategy only focuses on the operation of IFCs under unbalance condition and protects IFC from the adverse effects by canceling out output power oscillations [70]–[72] and controlling output peak current [61], [73].

In both control options, the IFC is modeled as a virtual negative sequence impedance Z^- in the negative sequence circuit, and it is controlled to achieve the control objectives. In details, the virtual negative sequence impedance can be controlled to be much smaller than the grid impedance, directing unbalance source negative current to flow into the IFC side and leading to an improved PCC voltage. However, how the control of IFC virtual negative sequence impedance can minimize the IFC's output active power oscillation and effectively reduce the negative sequence voltage of PCC are addressed in the two control strategies.

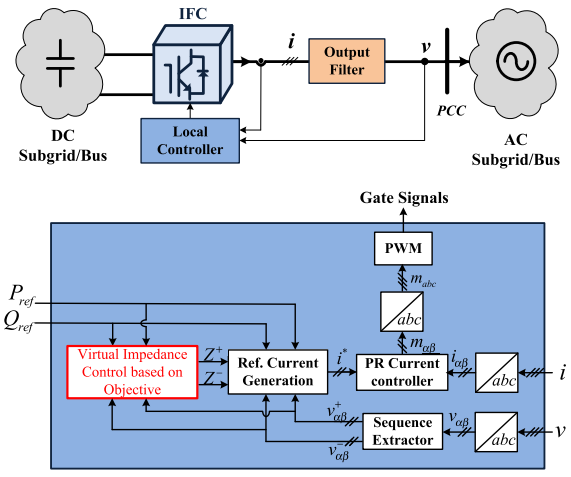

FIGURE 4. Typical individual three-phase IFC with control block diagram under unbalance voltage.

Based on the desired objective, the IFC's virtual impedance is usually determined in the secondary controller. Then, the impedances are used to update the reference current of IFC in the primary controller for unbalance condition compensation. The primary control of IFC is usually CCM. In Fig. 4, a typical individual three-phase IFC with control block diagram under unbalance voltage is shown. In this figure, the primary and secondary controllers are run in the local controller of the IFC.

Control Strategy Example of Three-Phase IFC for Adjustable Compensation of PCC Unbalance Voltage with IFC Active Power Oscillation Minimization

In this example, it is assumed that three-phase IFC is connected to the AC subgrid at the PCC. To adjustably compensate for the unbalanced voltage and control IFC's output power oscillation, both IFC's positive and negative sequences current should be controlled. In this example [65], the reference current in (1) is considered in which k_1 and k_2 are defined as $k_1 = P^+_{ref}/P_{ref}$ and $k_2 = Q^+_{ref}/Q_{ref}$ to adjust positive and negative sequences of active and reactive currents. Here, P_{ref} and Q_{ref} are the reference average active and reactive powers of the IFC, and the P^+_{ref} and Q^+_{ref} are the positive sequences of the P_{ref} and Q_{ref}. The k_1 and k_2 can be used to compensate for unbalanced voltage as well as control IFC's output power oscillations, peak current, and DC link voltage ripples. In (1), i^* is the IFC's reference current, the v^+ and v^- are positive and negative sequence vector components of the three-phase PCC voltage vector, the i^+_p and i^-_p are the positive and negative sequence components of the active reference current, and the i^+_q and i^-_q are positive and negative sequence components of the reactive reference current.

$$i^* = \underbrace{\frac{P_{ref}\,k_1}{|v^+|^2}v^+}_{i^+_p} + \underbrace{\frac{P_{ref}\,(1-k_1)}{|v^-|^2}v^-}_{i^r_p} + \underbrace{\frac{Q_{ref}\,k_2}{|v^+|^2}v^+_\perp}_{i^+_q} \underbrace{\frac{Qref\,(1-k_2)}{|v^-|^2}v^-_\perp}_{i^r_q} \quad (1)$$

From (1), the sequential model of the system can be achieved as in Fig. 5 [65] (three-phase three-wire system, which doesn't have a zero sequence component).

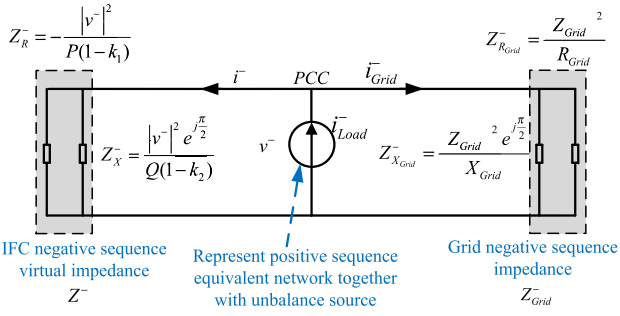

FIGURE 5. Negative sequence model of three-phase IFC connected to the AC subgrid.

To adjustably compensate for the unbalanced voltage (negative sequence voltage control), the IFC's negative sequence current amplitude is controlled, which can be achieved

from (1) and Fig. 5 as follows:

$$\left|i^{*^-}\right| = \frac{\left|v^-\right|}{\left|Z^-\right|} = \sqrt{\left(\frac{P_{ref}(1-k_1)}{\left|v^-\right|}\right)^2 + \left(\frac{Q_{ref}(1-k_2)}{\left|v^-\right|}\right)^2} \tag{2}$$

where i^{*^-} is the IFC's negative sequence reference current and Z^- is virtual negative sequence impedance. Also, the IFC's output active power oscillations at the PCC can be achieved from (1), and the following objective function is defined to minimize it:

$$\left[\left(\frac{P_{ref}k_1}{\left|v^+\right|^2} + \frac{P_{ref}\,(1-k_1)}{\left|v^-\right|^2}\right)\left|v^+\right|\left|v^-\right|\right]^2 + \left[\left(\frac{Q_{ref}k_2}{\left|v^+\right|^2} - \frac{Q_{ref}(1-k_2)}{\left|v^-\right|^2}\right)\left|v^+\right|\left|v^-\right|\right]^2 \tag{3}$$

Thus, the objective function in (3) is minimized subjected to the constraint in (2) using the Lagrangian method [65]. From this method, k_1 and k_2 are calculated analytically as a function of the system operating point, and they can be easily updated in a digital controller on-line (see Fig. 4).

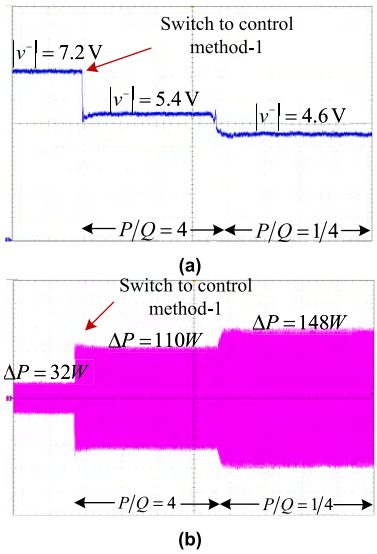

FIGURE 6. Performance of the PCC unbalanced voltage compensation and IFC's active power oscillation minimization; (a) negative sequence voltage of the PCC, and (b) IFC's active power oscillation [65].

The performance of the control strategy under different power factors of IFC in the inductive grid is verified, and the results are shown in Fig. 6. In the results, before applying the control method to the three-phase IFC, $k_1 = k_2 = 1$, where just positive sequence active and reactive currents are injected to the grid without any compensation (see (1)). After applying the control method, the negative sequence voltage is reduced (unbalanced voltage is compensated), and the active power oscillation is minimized in that operating point.

B. CONTROL OF PARALLEL THREE-PHASE IFCS UNDER UNBALANCED VOLTAGE

In some research, the parallel IFCs are referred to converters without a common DC link connected to the same AC subgrid. In such systems, the control strategies are focusing on unbalanced voltage compensation without considering its adverse effects on IFCs operation [51], [74]–[78]. In case that output power/current of DGs/SEs connected to the AC subgrid are high, parallel IFCs with common DC link are used. Also, the parallel IFCs are used to interlink AC and DC subgrids where high power/current is planned to be exchanged or high reliability is required. In the parallel IFCs with common DC link, adverse effects of unbalanced voltage on the IFCs operation are aggregated (IFCs' active power oscillation (ΔP), DC link ripples, and peak current increase could be amplified). However, if controlled properly, individual IFC's adverse effects might cancel out each other. To improve both the AC and DC subgrids power quality, active power oscillation cancellation with peak current control are desirable [79]–[81]. The control strategies are classified into two groups:

- **One dedicated IFC focusing on ΔP cancellation:** One interfacing converter, named as redundant IFC, cancels out active power oscillations of the other IFCs (the redundant IFC produces 180-degree out-of-phase active power oscillation compare to the other IFCs), while all IFCs peak currents are also controlled not to exceed their rating limits [79], [80].
- **All IFCs participate in ΔP cancellation according to their power ratings:** The collective active power oscillations cancellation is shared among IFCs based on their available power ratings [81]. Similar to the first control option, peak currents of all IFCs are controlled not to exceed their rating limits.

Based on the desired objective, appropriate signals are generated in the supervisory control center (SCC). Then, the produced parameters are sent to primary controllers of IFCs to update reference currents (the primary controller of IFCs are usually CCM). For closely located IFCs, a local controller of one of IFC can be used as SCC (master-slave structure of SCC, see Fig. 3). In Fig. 7, the parallel IFCs with control block diagram under unbalanced voltage are shown. In this figure, it is assumed that the supervisory control center has a centralized structure.

Control Strategy Example of Parallel Three-Phase IFCs with all IFCs Participate in ΔP Cancellation

In this example, it is assumed that the parallel IFCs with common DC link connects the AC and DC subgrids, as shown in Fig. 7. In this control strategy [81], all parallel IFCs, which are operated under unity power factor (PF), are participating in active power oscillations cancellation to provide an oscillation-free DC link. Also, the collective peak current of n-parallel IFCs (it is a constant value under $\Delta P = 0$ and fixed average active and reactive powers) is shared among IFCs according to their ratings. This control strategy also

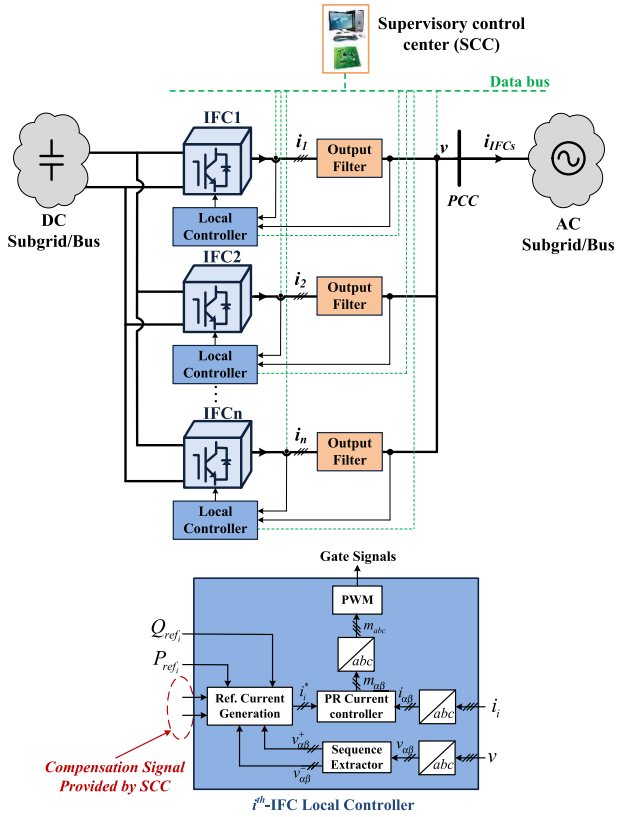

FIGURE 7. Typical parallel three-phase IFCs with control block diagram under unbalance voltage and centralized structure of supervisory control center.

maximizes power/current transferring capability of IFCs by minimizing the peak current of each IFC.

To easily control the adverse effects of unbalance voltage on IFCs' operation, i^{th}-IFC's reference current under unity PF operation is considered as in (4) [81]–[83].

$$i^*_{P_i} = i^{*+}_{Pi} + i^{*-}_{Pi} = \frac{P_{ref_i}}{|v^+|^2 + k_{p_i}|v^-|^2} v^+ + \frac{P_{ref_i} k_{p_i}}{|v^+|^2 + k_{p_i}|v^-|^2} v^- \quad (4)$$

where i^{*+}_{Pi} and i^{*-}_{Pi} are positive and negative sequence components of i^{th}-IFC's reference current vector under unity PF operation, k_{pi} is the scalar coefficient which is defined to cancel out active power oscillation of the IFCs, P_{ref_i} is the average output active power of i^{th}-IFC, and v^+ and v^- are positive and negative sequence vector components of the three-phase PCC voltage vector. From (4), the i^{th}-IFC's instantaneous output active power can be achieved as follows (three-phase, three wire power systems):

$$p_i = \left(\underbrace{v^+ \cdot i^+_{Pi}}_{P^+_{refi}} + \underbrace{v^- \cdot i^-_{Pi}}_{P^-_{refi}} \right) + \left(\underbrace{v^+ \cdot i^-_{Pi} + v^- \cdot i^+_{Pi}}_{\Delta P_i} \right)$$
$$= P_{ref_i} + \frac{P_{ref_i}(1 + k_{p_i})(v^+.v^-)}{|v^+|^2 + k_{p_i}|v^-|^2} \quad (5)$$

where p_i is the instantaneous output active power of the i^{th}-IFC, P^+_{refi} and P^-_{refi} are the positive and negative sequences of i^{th} -IFC's average active power, and ΔP_i is the oscillating output active power of i^{th} -IFC. Considering (5), $k_{pi} = -1$ results in i^{th}-IFC's active power oscillation cancellation, which provides a much easier way compared to (3). From (5), to cancel out collective active power oscillation of n-parallel IFCs, following constraint should be satisfied [79]:

$$\Delta P = \sum_{i=1}^{n} \frac{P_{ref_i}(1 + k_{p_i})(v^+.v^-)}{|v^+|^2 + k_{p_i}|v^-|^2} = 0$$
$$\Rightarrow \sum_{i=1}^{n} \frac{P_{ref_i}}{|v^+|^2 + k_{p_i}|v^-|^2} = \frac{\sum_{i=1}^{n} P_{ref_i}}{|v^+|^2 - |v^-|^2} \quad (6)$$

Considering (4) and (6), the collective reference current vector of n-parallel IFCs under unity PF operation with zero collective active power oscillations ($\Delta P = 0$) is obtained as:

$$i^*_{IFCs}\big|_{\Delta P=0} = \frac{\sum_{i=1}^{n} P_{ref_i}}{|v^+|^2 - |v^-|^2} v^+ + \frac{-\sum_{i=1}^{n} P_{ref_i}}{|v^+|^2 - |v^-|^2} v^- \quad (7)$$

From (7), under $\Delta P = 0$, the current is independent from k_{pi} and is affected by $\sum_{i=1}^{n} P_{ref_i}$ variations. Thus, the collective peak current of n-parallel IFCs is a constant value under $\Delta P = 0$ and given P_{ref_i}, which results in the following conclusions [79], [81]:

- If all individual IFCs' peak currents are kept in the same phase as the collective peak current, their amplitudes' summation will be reduced.
- If all individual IFCs' peak currents are kept in the same phase and in-phase with collective peak current, their amplitudes' summation will be minimized (provides maximum power/current transferring capability).

As an example, assume that the collective peak current of n-parallel IFCs is in the phase c (among three phases a, b, and c). If all individual IFCs' peak currents are kept in the phase c, the summation of their amplitudes will be reduced. Also, if all individual IFCs' peak currents are kept in the phase c and in-phase with collective peak current (in-phase peak current vectors), their amplitudes' summation will be minimized. More information about the peak currents of parallel IFCs can be found in [81].

Considering i^{th}-IFC's reference current of (4), it can be proven that if $k_{pi} < 0; i = 1, \ldots, n$, all individual IFCs' peak currents would be in the same phase with the collective peak current of parallel IFCs [79], [81]. Also, the difference between phase angles of individual i^{th}-IFC peak current and n-parallel IFCs collective peak current under $\Delta P = 0$ in unity PF operation is small enough, and they can be considered in-phase with a good approximation. Thus, all individual IFCs peak currents are in the same phase and approximately in-phase with the collective peak current of parallel IFCs under unity PF if $k_{pi} < 0; i = 1, \ldots, n$.

In this control example, the following expressions are solved to calculate the k_{pi} of all IFCs, where I^{max}_{pi} is peak current of i^{th}-IFC, obtained from (4), and U_i and S_i are sharing

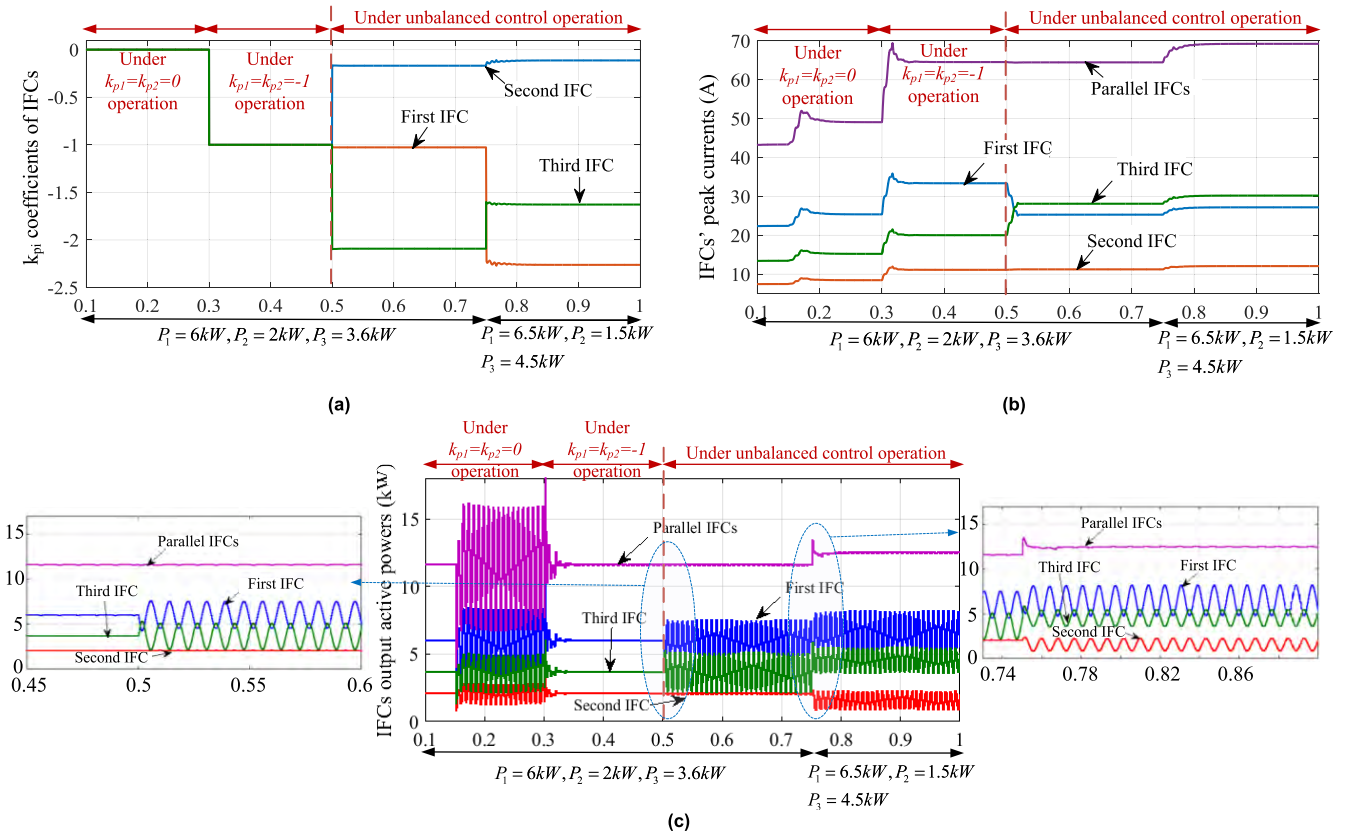

FIGURE 8. Simulation results of 3-parallel IFCs under unbalance condition when all IFCs participate in ΔP cancellation; (a) k_{pi} coefficient factors, (b) IFCs' output peak currents, and (c) IFCs' output active powers [81].

factor and power rating of i^{th}-IFC [81]:

$$\sum_{i=1}^{n} \frac{P_{ref\,i}}{|v^+|^2 + k_{p_i}|v^-|^2} = \frac{\sum_{i=1}^{n} P_{ref\,i}}{|v^+|^2 - |v^-|^2} \tag{8}$$

$$U_1 I_{p1}^{max} = U_2 I_{p2}^{max} = \ldots = U_n I_{pn}^{max} \tag{9}$$

$$U_i = \frac{S_1}{S_i} \quad i = 2, \ldots, n \tag{10}$$

$$k_{pi} < 0 \quad i = 1, \ldots, n \tag{11}$$

In this control strategy, (8) provides zero collective active power oscillation (see (6)), (9) and (10) guarantee collective peak current sharing of IFCs based on their ratings, and (11) maximizes power/current transferring capability of IFCs. This set of equations should be solved in the supervisory control center to achieve the k_{pi} of all IFCs.

The performance of this control strategy is verified, and the results are provided in Fig. 8 (3-parallel IFCs are tested). After applying the unbalance condition at $t = 0.3s$, first, zero active power oscillations of IFCs are provided by setting the $k_{p1} = k_{p2} = k_{p3} = -1$. Since the parallel IFCs' collective peak current is not shared between them based on their power ratings, this control method is applied. Considering the results, it is clear that all IFCs peak currents are kept in the same phase with the collective peak current of parallel IFCs to maximize power transferring capability ($k_{pi} \leq 0$), the collective peak current is shared among parallel IFCs based on their power ratings ($S_1 = 9\ kVA, S_2 = 4kVA, S_3 = 10kVA$), and collective active power oscillation is zero.

C. CONTROL OF SINGLE-PHASE IFCS UNDER UNBALANCE VOLTAGE

In the hybrid microgrids, single-phase IFCs are used to connect single-phase DGs/SEs to AC subgrid or to interlink DC subgrids and single-phase AC subgrids. Due to the high penetration level of such IFCs, they can be coordinated for unbalancing condition compensation of three-phase AC subgrids. There are two control options for active compensation of unbalance condition:

- **IFCs active and reactive powers control for unbalance compensation:** The single-phase IFCs' output active and reactive powers are controlled to adjustably compensate for the unbalanced condition [84]–[87].
- **IFCs reactive powers control for unbalance compensation:** Reactive powers of single-phase IFCs are controlled for adjustable compensation of unbalance condition, and the active powers of IFCs are controlled for power management purposes [84], [88].

In both aforementioned control options, the supervisory control center (SCC) provides the reference average powers to the primary controllers of the IFCs. The primary controller updates the reference currents of IFCs for

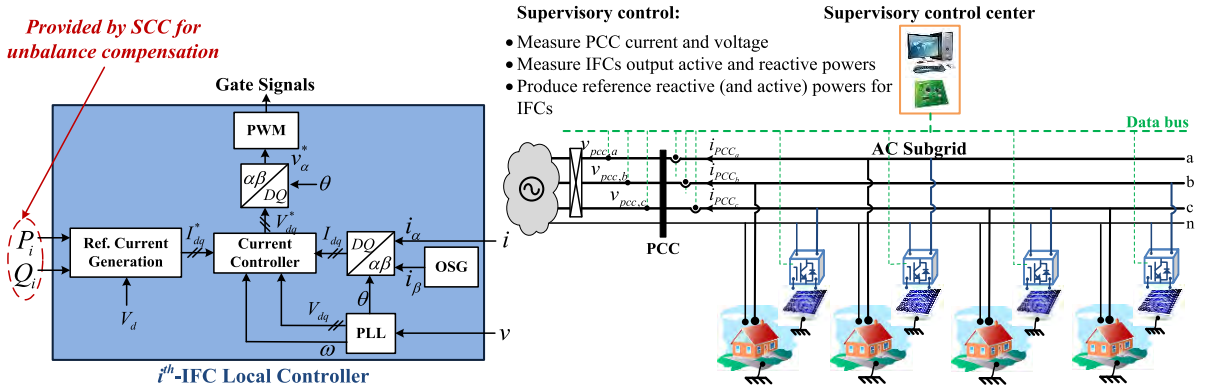

FIGURE 9. A typical example of control of single-phase DGs' IFCs connected to the AC subgrid for unbalance compensation.

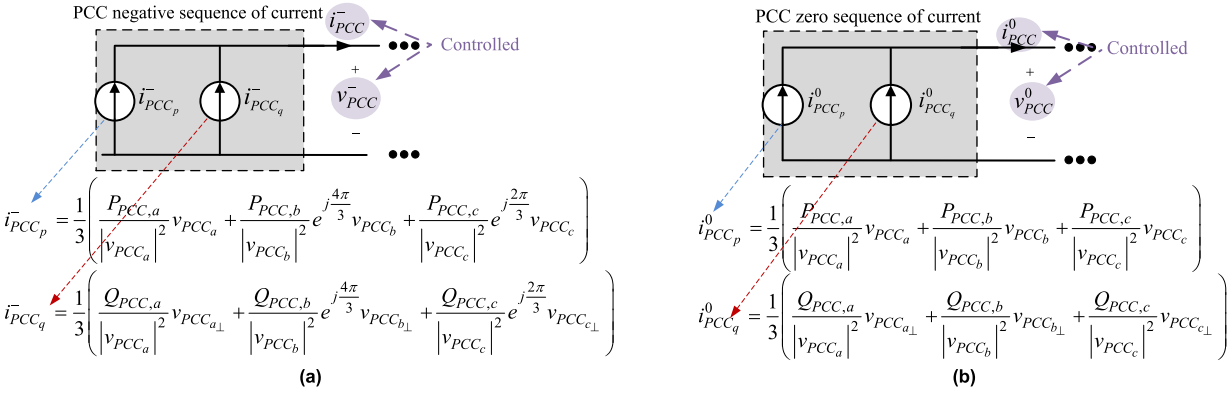

FIGURE 10. Negative and zero sequence models of the AC subgrid seen from the PCC.

compensation purposes. It should be mentioned that the SCC usually has a centralized structure, and the primary controller of IFC is CMM. In Fig. 9, a typical example of single-phase IFCs connected to the AC subgrid is shown.

Control Strategy Example of Single-Phase IFCs for Unbalance Compensation of Three-phase AC Subgrid using Reactive Powers of IFCs

In this example [84], a power system similar to Fig. 9 is considered, where the total reference current of phase-x at the PCC from single-phase perspective could be defined as:

$$i_{PCC_x} = \underbrace{\frac{P_{PCC,x}}{|v_{PCC_x}|^2} v_{PCC_x}}_{i_{PCCxp}} + \underbrace{\frac{Q_{PCC,x}}{|v_{PCCx}|^2} v_{PCC_{x_\perp}}}_{i_{PCCxq}} \quad x = a, b, c \tag{12}$$

where i_{PCC_x} is the total reference current of PCC in phase-x, $i_{PCC_{xp}}$ is an active current of PCC in phase-x, $i_{PCC_{xq}}$ is a reactive current of PCC in phase-x, v_{PCC_x} is the three-phase PCC voltage vector, $v_{PCC_{x_\perp}}$ lags v_{PCC_x} by 90°, and $P_{PCC,x}$ and $Q_{PCC,x}$ are the average active and reactive powers of PCC in phase-x. The active and reactive currents generate the active and reactive powers in three phases, respectively.

From (12), the negative and zero sequence models of the system seen from the PCC can be achieved (since it is a 4-wire power system, zero sequence components will not be zero), which are shown in Fig. 10 [84]. As clear from the figures, the negative sequence and zero sequence currents (i^-_{PCC} and i^0_{PCC}) can be decomposed into active terms and reactive terms. Since only reactive powers control for unbalance compensation is desired, the $i^-_{PCC_q}$ and/or $i^0_{PCC_q}$ can be controlled to absorb the constant $i^-_{PCC_p}$ and/or $i^0_{PCC_p}$ to minimize the i^-_{PCC} and/or i^0_{PCC}, respectively.

Considering Fig. 10, the objective function for compensation of negative and zero sequences currents can be achieved, as provided in (13). Since the reactive powers in three phases are control variables in both negative and zero sequences currents compensations, controllable weighting factors (k^- and k^0) are defined for flexible compensation of negative and zero sequences current and keeping them in their desired level. For example, when $k^- = 1 (k^0 = 0)$, three variables $Q_{PCC,a}$, $Q_{PCC,b}$, and $Q_{PCC,c}$ are controlled to minimize the negative sequence current; otherwise $k^- = 0 (k^0 = 1)$ leads to minimization of zero sequence current. In case that $k^- \neq 1$ and $k^0 \neq 1$, both negative and zero sequences current are compensated in which their compensation levels

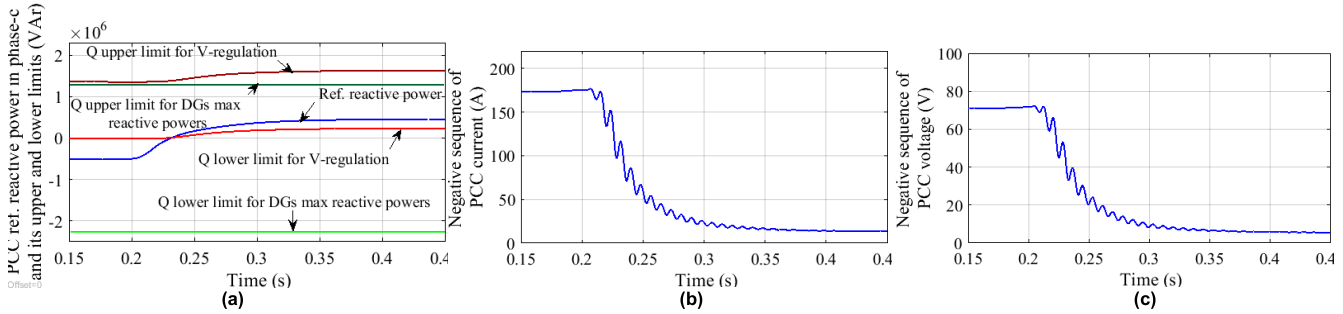

FIGURE 11. Performance of negative sequence current compensation ($k^- = 1; k^0 = 0$) using single-phase IFCs; (a) reference reactive power in phase-c at the PCC and its boundary limits, (b) negative sequence current at the PCC, and (c) negative sequence voltage at the PCC [84].

TABLE 1. Summary of unbalanced compensation in hybrid AC/DC microgrids using IFCs.

Unbalance Compensation in Hybrid AC/DC Microgrids by Interfacing Converters (IFCs)						
Three-Phase IFCs					Single-Phase IFCs	
Individual IFCs			Parallel IFCs		(5) IFCs active and reactive powers control for unbalance compensation:	(6) IFCs reactive powers control for unbalance compensation:
(1) Active compensation of unbalanced voltage		(2) Control of unbalance voltage adverse effects on IFC operation:	(3) One dedicated IFC focusing on ΔP cancellation:	(4) All IFCs participate in ΔP cancellation:		
(1.1) Adjustable compensation and adverse effect control:	(1.2) Adjustable compensation without direct control of adverse effect:					
- Direct control of IFC's active power oscillation and/or its peak current - Adjustable unbalance voltage compensation - Less max unbalance compensation level than (1.2)	- No direct control of IFC's active power oscillation and/or its peak current - Only focus on unbalanced voltage compensation - More max unbalance compensation level than (1.1)	- No direct control of unbalanced voltage compensation - Focus on operation of IFCs under unbalance condition - Less max unbalance compensation level than (1)	- One IFC cancel out active power oscillation of other IFCs - All IFCs peak currents control not to exceed their rating limits - Power rating of redundant IFC should be large enough	- Sharing collective active power oscillation cancellation among IFCs based on their available power ratings - All IFCs peak currents control not to exceed their rating limits - No need for IFC as redundant with high power rating (see (3)) - Higher computational burden than (3)	- Larger max unbalance compensation level than (6) - Active powers can not be controlled for power management. - May not be cost effective due to active power restrictions (e.g. PVs may not work on MPPT)	- Smaller max unbalance compensation level than (5) - Active powers are controlled for power management purposes.

are determined by k^- and k^0.

$$F\left(Q_{PCC,a}, Q_{PCC,b}, Q_{PCC,c}\right) = k^- F_1\left(Q_{PCC,a}, Q_{PCC,b}, Q_{PCC,c}\right) + k^0 F_2\left(Q_{PCC,a}, Q_{PCC,b}, Q_{PCC,c}\right) \quad k^- + k^0 = 1 \tag{13}$$

In (13), the F_1 and F_2 are three-variables quadratic objective functions for compensation of negative and zero sequences current, respectively [84].

In this optimization problem, two constraints are considered: three-phase voltage restriction between upper and lower limits [89], [90], and available power rating limits of IFCs for compensation purposes. The developed optimization problem is minimized using the KKT method, in which systems of 3 linear equations with 3 variables are obtained. Owing to their simplicity, the equations can be solved online easily, and reference reactive power in each phase at the PCC can be achieved. Then, the reference reactive power at each phase is shared among the IFCs in that phase considering their available ratings.

This control strategy is applied to IEEE 13-node test system [91], in which seven single-phase DGs are integrated into different buses, and they are used to compensate for the negative sequence current at the PCC ($k^- = 1$ and $k^0 = 0$). The results are shown in Fig. 11. As seen from the results, after applying the control strategy at $t = 0.2$, the negative sequence current is reduced from $173A$ to $13A$, and the negative sequence voltage at the PCC is reduced from $71V$ to $5V$.

In Table 1, presented control strategies of IFCs for unbalanced condition compensation in Section IV, as well as their strengths and challenges, are summarized.

V. HARMONIC COMPENSATION IN HYBRID AC/DC MICROGRIDS THROUGH INTERFACING CONVERTERS

In both DC and AC subgrids, the presence of nonlinear loads and the switching mode power converters make the harmonic

pollution a significant concern. These harmonics, particularly the low-order harmonics, can cause extra losses, interferences to the grid-connected apparatus, and even resonances in the microgrid [7], [92]–[94]. To mitigate the harmful harmonics, both passive power filters (PPFs) and active power filters (APFs) can be used to provide low-impedance paths for harmonics, improving the power quality of the other nodes in the microgrid. However, installing dedicated filters (passive or active) require extra cost, and they are not that effective since the harmonics' sources are widely distributed.

Thanks to the development of IFCs' control strategies, the harmonic compensation has been added as ancillary functions to the interfacing converters in both AC and DC subgrids. Thus, the harmonics can be mitigated in both AC and DC subgrids in a distributed manner without extra cost.

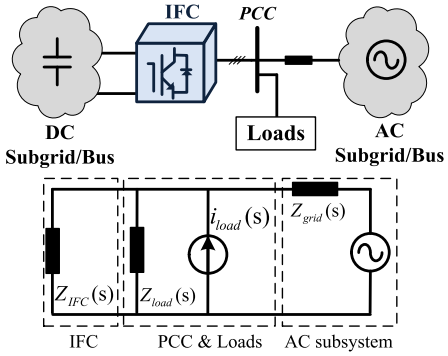

FIGURE 12. The equivalent circuit of IFC connected to AC subgrid.

A. CONTROL OF IFCS FOR HARMONIC COMPENSATION IN AC SUBGRID

The AC subgrid voltage distortion is mainly caused by the nonlinear loads, particularly in a weak grid. As can be seen from Fig. 12, the nonlinear loads inject harmonic current into the system, and the PCC voltage will be distorted when the harmonic current flows through the high impedance of the grid. If the nonlinear loads current can be absorbed by the IFC, the voltage distortion can be mitigated. This requires the IFC to decrease the output impedance at the harmonic orders, which can be done by increasing the loop gain of the IFC's controller. The most popular way is adopting specific controllers such as resonant controllers, repetitive controllers, and deadbeat controllers in the feedback loops.

- **Resonant Controller (RSC):** The RSC has theoretically infinite gain at the resonant frequency [95]. Simply setting the resonant frequency at the harmonic orders and connecting multiple RSCs in parallel can realize selective harmonic control [96]. The control gains of each harmonic control branch can be flexibly tuned. However, the computation burden and design complexity can be very high when a wide range of odd-order harmonics are required to be mitigated. Also, the phase margin of the system becomes small when multiple RSC is applied [97]–[99]. To reduce the number of RSCs required for harmonic control, the RSCs can be applied in the synchronous frame. In this case, for example, 6^{th} order RSC can be used to control 5^{th} and 7^{th} order harmonics. As a result, the number of required RSCs can be halved [100], [101]. Another challenge is the grid frequency variation [98], [99], particularly in the weak grid or islanded microgrids. To resist the frequency variation, the RSC can be improved by adaptive resonant frequency [102] or adding damping term to the denominator of the RSC [102], [103], expanding frequency range that provides high loop gain.
- **Repetitive Controller (RC):** The RCs, featuring simple structures, can introduce multiple resonance peaks at integer times of the center frequency in the spectrum, which enable the mitigation of wide-range of harmonics at the integer orders; odd orders [104], [105], or even selected orders [106]–[109]. Compared to RSC, the RC requires more memory to store delayed signals, but much less calculation time, which is quantized in [110]. The delay embedded in the controller degrades the transient performance. Moreover, it is difficult to define different loop gains at different harmonic orders, which is important to reshape harmonic impedances for harmonic sharing or stability enhancement. Similar to the RSC, the tracking error of RC is also inevitably affected by the frequency deviation, requiring frequency adoption manners [111]–[114].
- **Deadbeat (DB) Controller:** The DB controllers can achieve fast transient and wide-range harmonics control with no special request on calculation capacity or memory. In addition to the harmonics at specific orders, the inter-harmonics can also be controlled. However, the complexity of the DB controller in high-order systems can be a demerit, such as IFCs with LCL filters. In addition, the tracking error is influenced by the variation of system parameters, system delay, dead time, and the error between the stepwise sampling results in digital controllers and the actual continuous system outputs. To address these challenges, different researches have been done to reduce complexity [115], reduce system delay and sampling error [116], compensate the dead-time [117], avoid model mismatch [118]–[121], to name a few.

These aforementioned controllers can be selected according to the requirement of the harmonic control. These controllers can be implemented in three different control methods of the IFCs: current control method (CCM), voltage control method (VCM), and hybrid control method (HCM). In following, these control options in accompany with implementation examples are explained.

1) HARMONICS COMPENSATION WITH CURRENT CONTROL METHOD (CCM)

The interfacing converter with CCM has high impedance at the fundamental frequency as the converter behaves like a current source (see Fig. 2), and it is convenient to add harmonic

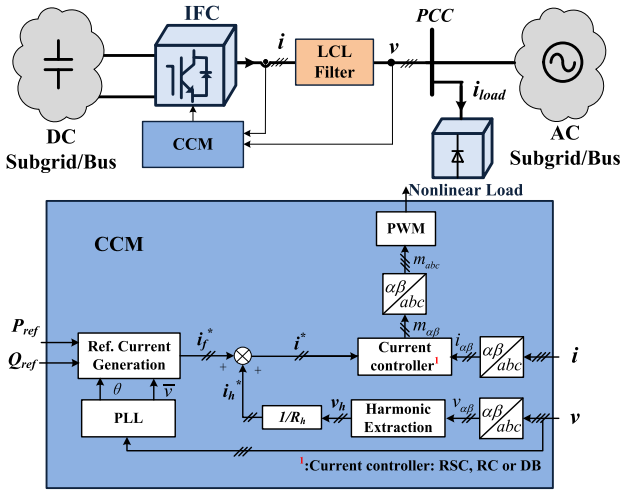

FIGURE 13. A typical individual IFC control block diagram with CCM harmonic compensation.

controllers to mitigate harmonics [122]–[126]. With the harmonic controllers, the current reference is generated according to the control targets. In general, there are two control targets:

- **Reject current harmonics at the output of IFC:** A pure sinusoidal current reference will be applied to the harmonic controllers to eliminate IFC's output current harmonics [125]–[127].
- **Compensate PCC voltage harmonics:** The IFC should be controlled as a shunt active power filter to absorb current harmonics [122]–[124], [128].

In Fig. 13, a typical individual IFC's control block diagram with CCM harmonic compensation is shown.

Control Strategy Example of IFC for Harmonics Compensation of PCC Voltage with CCM

In this example [124], the IFC connected to the AC subgrid at the PCC is used to compensate harmonics with CCM. As seen in Fig. 13, the fundamental current reference i_f^* in CCM is derived by the output power control while the harmonic current reference i_h^* is calculated by the PCC voltage harmonics v_h and a virtual resistor R_h. Then, the current reference i^* can be obtained as follows:

$$i^* = i_f^* + i_h^* = i_f^* + v_h/R_h \tag{14}$$

In (14), the virtual resistor R_h is the output impedance of the IFC at the harmonic orders. Thus, the harmonic currents of the nonlinear loads are absorbed by the IFC to compensate for the PCC voltage harmonics. With RSC, RC, or DB controllers applied as the current controller, the harmonic compensation reference can be executed. The performance of the control strategy is shown in the results of Fig. 14, in which the PCC voltage is significantly improved with the CCM-based harmonic control.

Compared to directing the load harmonic current to the current reference and absorbing all the harmonic current of the nonlinear load ($R_h = 0$), the aforementioned control strategy can flexibly define the harmonic compensation efforts according to the IFC available power rating. This also enables harmonic current sharing among multiple IFCs by tuning R_h.

2) HARMONICS COMPENSATION WITH VOLTAGE CONTROL METHOD (VCM)

In the VCM-based method (see Fig. 2), the harmonic sharing and compensation can be obtained in the isolated operation mode [130]–[132], in the grid-connected operation mode [129], [133], [134], and in the unified control under both grid-connected and islanded conditions [135]–[137]. Another advantage of VCM-based harmonic compensation is the ability to follow given voltage amplitude and frequency

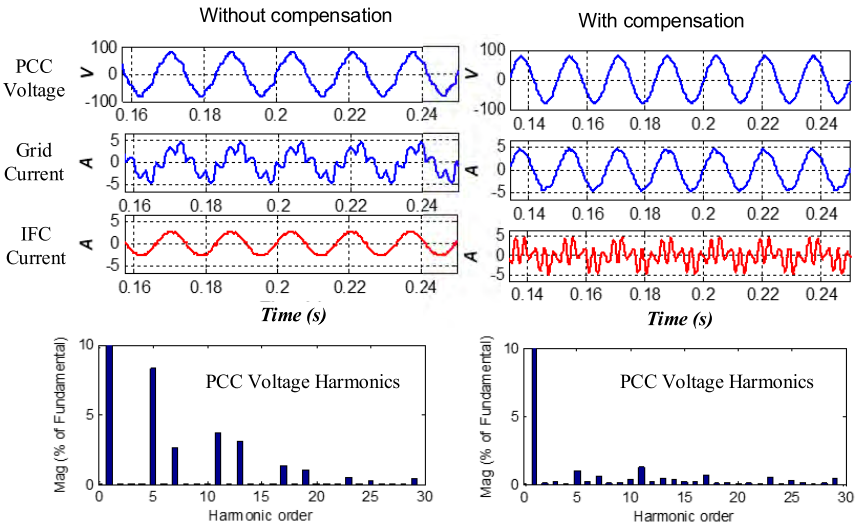

FIGURE 14. Performance of CCM-based control strategy of IFC for AC subgrid voltage harmonics compensation [129].

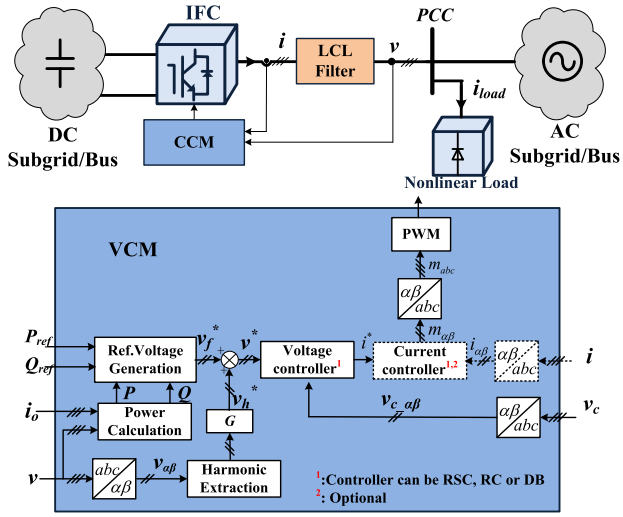

FIGURE 15. A typical individual IFC control block diagram with VCM harmonic compensation.

references from droop controller [130], [138] or virtual synchronous generator controller [139]–[141].

Generally, an RSC, RC, or DB controller can be used as the voltage controller to directly regulate the IFC output voltage. To obtain better dynamics, an inner current loop which regulates the inverter-side current can be added. However, as the grid-side current is not controlled in VCM, it is sensitive to PCC voltage disturbances. A typical individual IFC's control block diagram with voltage control method harmonic compensation is shown in Fig. 15.

Control Strategy Example of IFC for Harmonics Compensation of PCC Voltage with VCM

In this example [129], the PCC voltage harmonics are feed-forwarded to the voltage control reference with a gain G, similar to Fig. 15. The equivalent harmonic impedance Z_{IFC_eq} at the converter side can be expressed as:

$$Z_{IFC\_eq} = Z_{IFC}/(1+G) \tag{15}$$

where the Z_{IFC} is the original impedance without harmonic compensation and the G is feed-forward gain. When the feed-forward gain G is positive, the harmonic can be absorbed by the IFC (nonlinear load currents will flow to converter), while a negative gain G will lead the nonlinear load current to the grid side due to the large impedance of IFC, enforcing sinusoidal output current, like [142]. The performance of this control strategy is evaluated, and the results under different feed-forward gains are shown in Fig. 16. As expected, the PCC voltage harmonics are reduced when the positive feed-forward gain is applied, while a negative gain ($G = -1$) increases the harmonic impedance and improves the IFC output current quality.

In general, when the VCM-based harmonic compensation is applied, the IFC works as an L-APF (an active power filter (APF) with pure inductive output impedance) as the IFC impedance and the grid impedance are mainly inductive at harmonic frequencies. However, it is possible to control the IFC to be an R-APF (an APF with pure resistive output impedance) because G can be a real, imaginary or complex number [143].

3) HARMONICS COMPENSATION WITH HYBRID CONTROL METHOD (HCM)

Compare to VCM and CCM, the HCM can simultaneously control the IFC's output voltage and current as the parallel

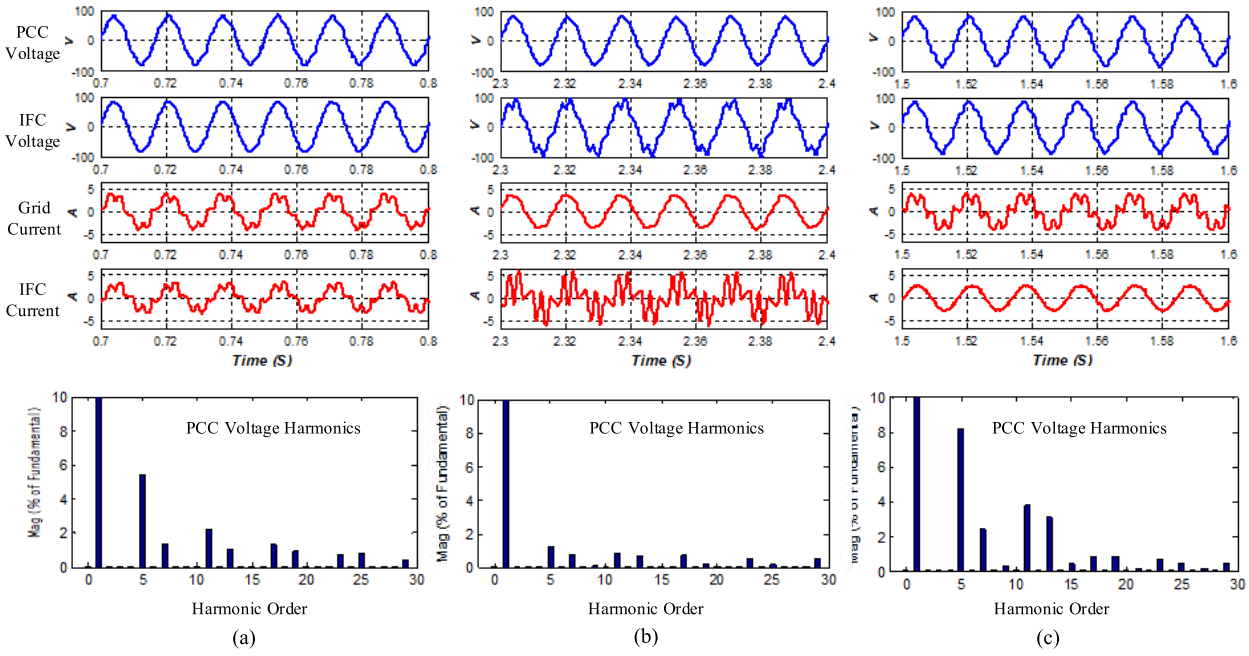

FIGURE 16. Performance of VCM-based harmonic compensation of IFC; a) G = 0, b) G > 0, and c) G = −1 [144].

control structure is used [144], [145]. In general, in VCM and CCM-based harmonic compensation, the converter-side inductor current control with a proportional controller is employed as the inner loop, and the outer voltage or current control loop (assuming LCL filter; to control capacitor voltage or grid-side current) usually uses multiple RSCs (with different resonant frequency) in parallel to control the harmonics (see Fig. 13 and Fig. 15). However, the HCM transforms the cascaded structure of a double-loop controller in CCM and VCM-based harmonic compensation into a single-loop parallel structure. In detail, there are two independent control branches in parallel in the HCM: closed-loop control of IFC's output voltage (filter capacitor voltage) and closed-loop control of current.

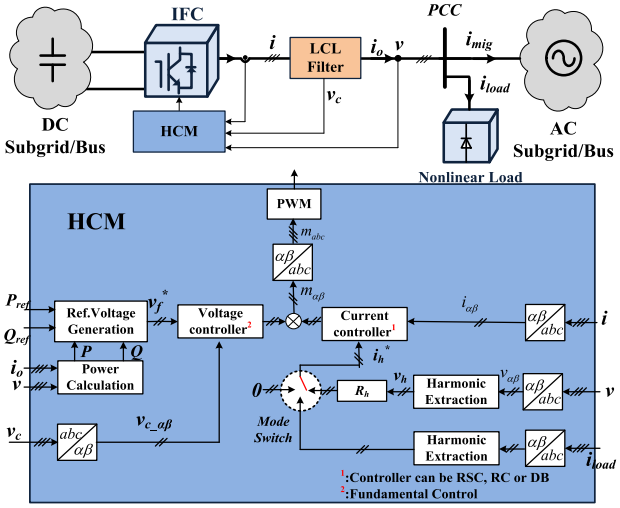

FIGURE 17. A typical individual IFC control block diagram with HCM harmonic compensation.

In Fig. 17, a typical harmonics compensation with HCM is shown. It is worth to note that the decoupling between the harmonic current branch and the fundamental voltage control branch can be achieved if the bandwidths of the control branches are properly designed. In HCM, the harmonic current can be controlled to achieve different objectives:

- **Compensate the PCC voltage harmonics:** If the current control reference is selected as $-H_D(s)V_{PCC}/R_V$, where R_V is the virtual resistance and $H_D(s)$ is the band-pass filter to extract the harmonics, the PCC voltage can be improved (see Fig. 17). The IFC works as a R-APF in this mode.
- **Reject the current harmonics:** The control target can also be set to reject the current harmonics. The harmonic current reference should be set to zero in this mode.
- **Compensate the local load's current harmonics:** If the current reference is selected as the current of local loads, the extracted harmonic components from local loads current can be directly used for the harmonic controller. This way, the microgrid injection current i_{mig} and PCC voltage v can be improved.

B. CONTROL OF LOW-SWITCHING IFCS FOR HARMONIC COMPENSATION IN AC SUBGRID

Typically, the interfacing converters for harmonic control usually have a switching frequency higher than 10KHz. However, in the high-power IFCs (≥500kW), low-switching frequency (<3KHz) is employed to reduce power loss. In such IFCs, the harmonic control performance is significantly affected by the control delay and low sampling rate, and the harmonic compensation is limited to low-order harmonics, such as 5^{th}, 7^{th} order harmonics. Therefore, it is preferable to perform the harmonic control with simple control structure instead of multiple-loop control. Also, the sampling rate can be increased while keeping low-switching frequency, requiring new sampling approaches to replace the well-accepted regular sampling method.

In the control system of low-switching IFCs, the above-mentioned VCM and CCM can only be applied for harmonic compensation when the inner current/voltage control loop employs controllers with fast transient and wide bandwidth, such as deadbeat (DB) control. Otherwise, HCM is more effective as the harmonics can be directly regulated, instead of feeding to cascaded inner control loops, which may degrade the transient performance and stability.

In addition to the feedback harmonic control strategies (CCM, VCM, and HCM), feed-forward paths aiming at harmonic mitigation can also be employed in low-switching IFCs. It is well known that adding a full feed-forward path of PCC voltage can help the IFCs resist the interference of the distorted PCC voltage and perform harmonic rejection [146]. In addition, more flexible harmonic control can be obtained by feed-forwarding PCC voltage or grid-side current to reshape the IFC output impedance, which enables flexible harmonic current rejection [147]–[150] and voltage harmonic compensation [150]. To achieve accurate impedance reshaping at desired harmonic orders, it is necessary to take system delay and feedback loop gains into consideration [150]. It is worth to note that the PCC voltages feed-forward based harmonic control strategies, which are in parallel to the current feedback loops, can also be variations of HCM. Therefore, the two methods have similar performance and design approaches.

Besides the control methods, the sampling method can also affect the harmonic control performance in low-switching IFCs. The widely applied regular sampling method limits the control sampling rate to be the same (symmetrical regular sampling) or twice (asymmetrical regular sampling) of the switching frequency. When the switching frequency is low (< 3kHz), e.g. in high-power grid-interfacing converters, the control sampling rate will be insufficient to accurately extract the harmonics. Also, the computation delay brought by the low-sampling rate will cause stability concerns. Therefore, new sampling methods should be used. In the following,

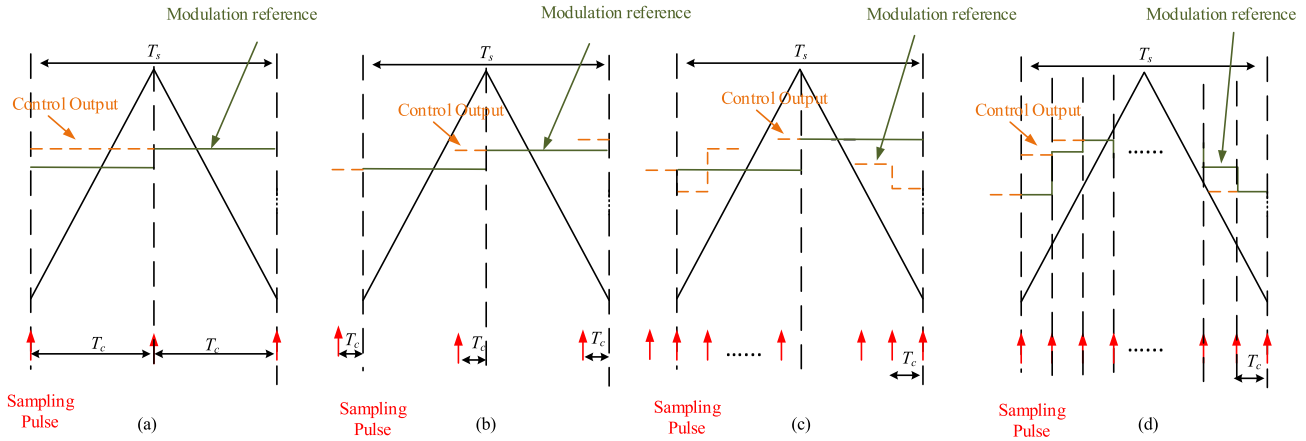

FIGURE 18. Different sampling methods: (a) asymmetrical regular sampling; (b) real-time computation method; (c) multi-rate method; (d) digital natural sampling method.

three different sampling methods are provided, which are compared with the asymmetrical regular sampling method in Fig. 18:

- **Real-time computation method** [151], [152]: The real-time computation method is shown in Fig. 18(b). Compared to the regular sampling method shown in Fig. 18(a), the sampling pulse is shifted forward for control computation. As a result, the modulation reference is generated by the newest available sampling results. The modulation reference is thus formed by real-time computation result. This way, the system delay is reduced while the harmonic sampling rate is still the same.
- **Multi-rate sampling method** [150]: The multi-rate method samples the control variables N times (N is an integer, N $>$ 2) of the PWM frequency (f_s) while the modulation reference is regularly sampled, as shown in Fig. 18(c). There are multiple sampling pulses in one PWM period. The system delay is thus reduced, and the sampling rate of harmonics is increased. In addition, the controller and the PWM are operated at different frequencies.
- **Digital natural sampling method** [153]: In digital natural sampling method, both the control sampling and PWM sampling are operated in high frequency, which is N times of the PWM frequency. As shown in Fig. 18(d), multiple sampling pulses are generated per PWM period, and the modulation reference will be updated with the same rate. Compared to the multi-rate sampling method, the PWM sampling rate is also increased. However, as modulation reference will be continuously updated, this sampling method may lead to multiple switching in one PWM period when the modulation reference has a similar slope with carriers, which is possible in harmonic control.

Control Example of Low-Switching IFCs for Harmonic Compensation with Feed-Forward Strategy and Multi-rate Sampling

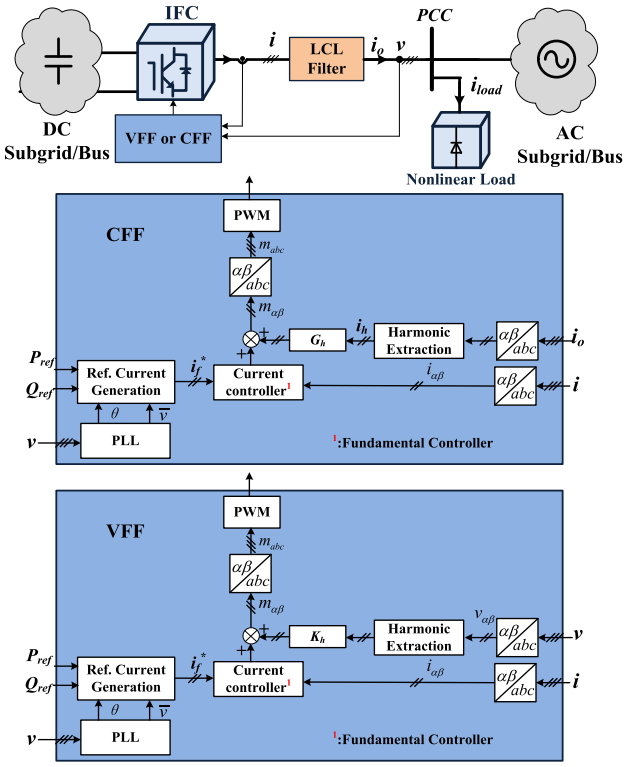

FIGURE 19. An example of harmonic control of low-switching IFCs with feed-forward strategies (current feed forward and voltage feed forward).

The two different feed-forward based harmonic control methods, current feed forward (CFF) method and voltage feed forward (VFF) method, are depicted in Fig. 19 [150]. In these two methods, the harmonic control signals are directly fed into the modulation references. Without cascaded multiple loop structure, the dynamics can be improved for low switching frequency converters. When the CFF path is added, the harmonic control gain plays the role of a virtual impedance in parallel with the original IFC's impedance. On the contrary, the VFF paths do not have

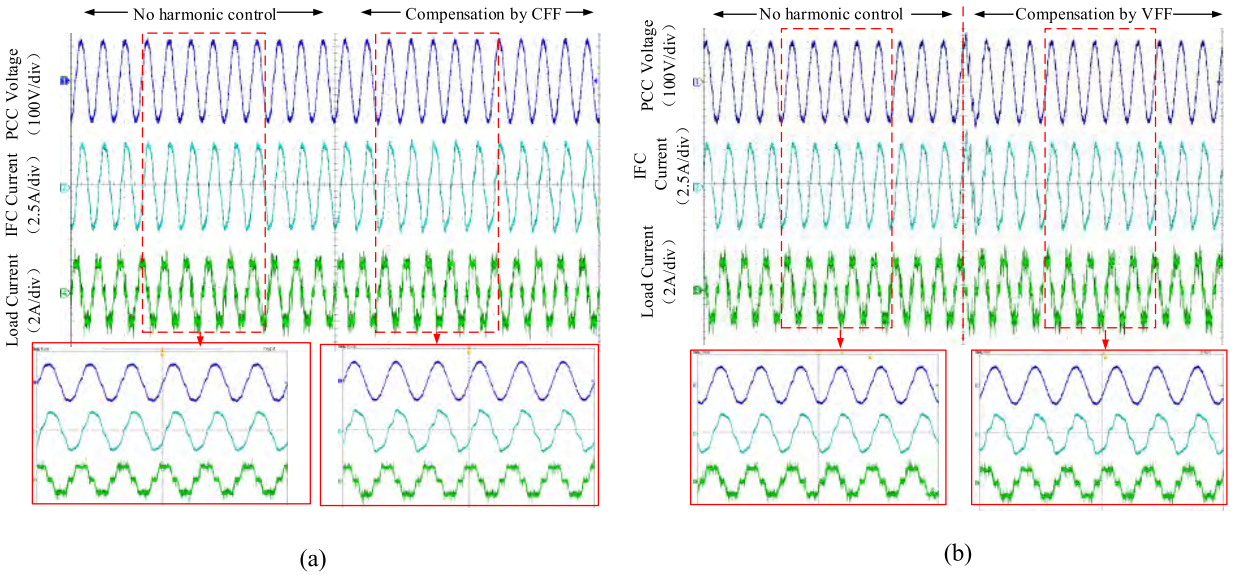

FIGURE 20. Performance of harmonic control of low-switching IFCs: (a) current feed-forward (CFF) method; (b) voltage feed-forward (VFF) method [150].

physical meanings, while the output impedance can be reshaped by the feed-forward gain. To address the challenges brought by low switching frequency, the multi-rate sampling method is applied. The sampling rate is set to be 20KHz and the switching frequency is 2KHz.

The control system performances are shown in Fig. 20. From the results, both methods (CFF and VFF) can effectively compensate for the distorted PCC voltage. By absorbing harmonics into the IFC, the PCC voltage becomes sinusoidal. However, the VFF method suffers from oscillations when the harmonic compensation is enabled, indicating the system becomes underdamped. On the contrary, the CFF, which is equivalent to adding paralleled impedances, shows smooth transient. It can be concluded that the CFF method is better in terms of stability.

C. CONTROL OF IFCS FOR HARMONIC COMPENSATION IN DC SUBGRID

In the hybrid AC-DC microgrids, the AC and DC subgrids have harmonic interactions due to the frequency coupling. The AC-side harmonics will be transferred to the DC side while the DC side ripple and harmonics will be transferred to the AC side through the IFC's PWM process [154]–[156]. In Fig. 21, the harmonic interaction between AC and DC subgrids are shown. The DC subgrids harmonics, particularly the low-order harmonics, are mainly introduced by the AC-side harmonics or unbalanced three-phase AC voltage. Also, the DC harmonics can be produced by DC-DC converters' control in the DC side such as maximum power point tracking control of PV systems [157], [158], or LC oscillation due to parasitic DC line impedance [159].

In the DC subgrid, since the DC-bus capacitors are usually large enough to ensure the reliable operation of DC subgrid under normal condition, high-frequency voltage ripples can

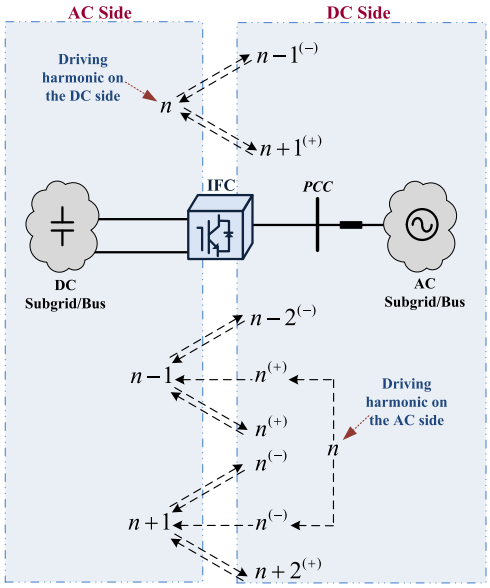

FIGURE 21. Harmonic interactions between AC and DC subgrids.

be easily filtered. Alternatively, the high-frequency harmonics can be easily filtered by tuned filters. For low-order harmonics, usually caused by AC subgrid, large capacitors or active power filters are required to mitigate harmonics. In practice, the 2nd order harmonic caused by the unbalanced AC voltage is the most important harmonic component to be addressed. Also, the 6th order harmonic may be observed due to the AC side 5th and 7th harmonics.

Similarly to the AC subgrid harmonics compensation, the interfacing converters provide a cost-effective option for the DC-subgrid harmonics compensation. In general, there are two control options:

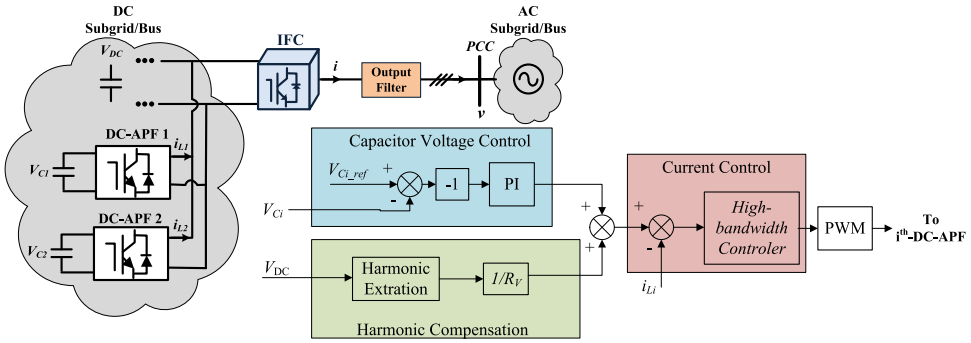

FIGURE 22. A typical example of two DC-DC IFCs control for DC-subgrid harmonic compensation.

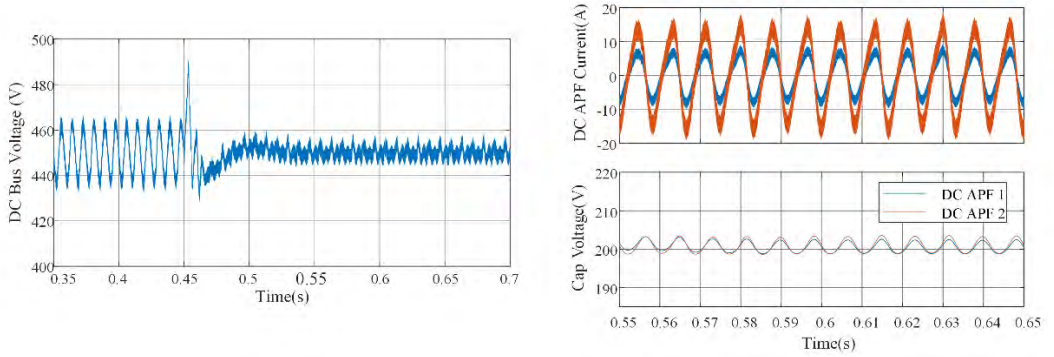

FIGURE 23. Performance of the two DC-DC IFCs control for DC-subgrid harmonic compensation; a) common DC bus voltage, b) DC-APFs output currents and their capacitor voltages.

- **Harmonics compensation using DC-AC interfacing converters:** The compensating 2nd order DC ripples usually leads to third-order harmonics in the AC side [66], [156], when the IFC exposes to unbalanced AC voltages and the control strategy has not been properly designed. Also, the methods focusing on improving the AC current quality under DC ripples while leaving the DC ripple unattenuated, such as directing the DC ripples to modulation references [160], are not applicable as well. Therefore, the major challenge is to simultaneously eliminate the 2nd-order DC voltage ripples while reducing 3rd-order harmonics at the AC side. Since the DC 2nd order ripples are usually caused by the unbalanced AC voltage, the current positive and negative sequence components can be controlled, which are widely used for unbalanced control [66], [161], [162]. These methods can reduce/mitigate active power oscillation (leads to reduce/mitigate 2nd order ripples at the DC side) and ensure AC current quality (for instance, see Section IV. A). As another alternative, the DC-AC IFCs can be paralleled to mitigate the 2nd-order harmonics in the DC side (active power oscillation cancellation in the AC side) according to their power rating. This way, the AC side current quality will not violate the grid codes if the DC ripple mitigation efforts are properly shared, which ensures the AC output quality [79]–[81].

- **Harmonics compensation using DC-DC interfacing converters:** In the hybrid AC-DC microgrids, harmonics on the DC side can be directly compensated by the DC-DC interfacing converters. The DC-DC IFCs, which can be named as DC-APFs in this condition, can compensate the low-frequency harmonics caused by both the AC-side and DC-side components. These converters provide a low impedance path for the harmonics (usually virtual resistor proportional to the power rating), directing the common DC link ripples and power/current oscillations to their own DC buses. Energy storage components, which can be capacitors, super-capacitors, batteries, etc., are required to absorb such oscillations. Moreover, to properly act as DC-APFs, it is required to use bidirectional DC/DC (BDC) converters, such as non-isolated half-bridge BDC [163] and isolated Dual Active Bridge (DAB) converter [159], [164]. In the hybrid AC-DC microgrid, distributed DC-APFs can be coordinated to share the harmonic compensation [164].

Control Strategy Example of DC-DC IFCs for Harmonics Compensation in DC Subgrid

In Fig. 22, an example of DC-subgrid harmonic compensation by two DC-APFs with different power ratings is provided. In the control strategy, the DC-APF capacitor voltage control and virtual resistor-based harmonic control are paralleled. The capacitor voltage control loop can ensure

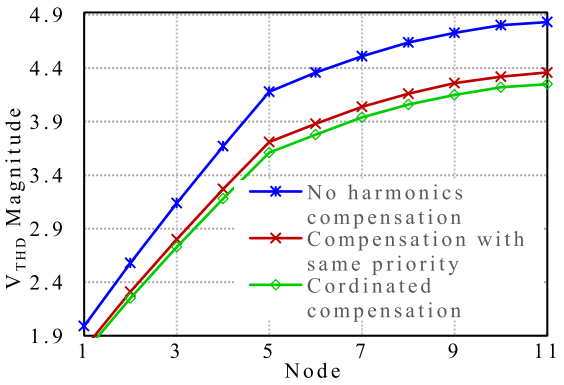

FIGURE 24. THD at each node under different compensation priority scheme [93].

the proper operation of the DC-APF, maintaining the average voltage on its low-voltage side capacitor. The compensation efforts are predefined according to the power rating of the DC-APFs. By sensing the voltage ripple on the DC bus, the DC APFs can control its input current to compensate the ripple. As a result, the 2nd order ripples are effectively mitigated. Also, thanks to the virtual resistor control, the ripple power is shared by the paralleled DC-APFs. As seen from the results in Fig. 23, the DC link oscillation is shared between the two DC-APFs with the ratio of 1:2, which is proportional to their power ratings. Also, the DC-APFs capacitor voltages are kept stable.

D. COORDINATED CONTROL OF MULTIPLE IFCS FOR HARMONICS COMPENSATION

In the hybrid AC-DC microgrids, the IFCs can be distributed throughout the system, requiring to collaborate control for the harmonic compensation. In detail, the harmonic compensation can be shared among the IFCs of the AC subgrid or DC subgrid based on their available rating, compensation priority, etc. In general, coordinate harmonic control strategies can be classified as:

- **Autonomous harmonic control:**The autonomous control enables the IFCs to collaboratively compensate harmonics without relying on communications. Similar to power-sharing control, the harmonic sharing can be achieved by adopting droop control (where the harmonic compensation efforts can be automatically determined by the harmonic droop gain proportional to the power ratings [165], [166]), by shaping the IFC output impedance [92], [131], [167]–[170], etc. However, similar to the reactive power sharing, the harmonic sharing can also be affected by the mismatched feeder impedance in the weak microgrid and differences in dynamic performance of converters, requiring some supervisory control to correct the sharing errors.
- **Supervisory harmonic control:** The supervisory harmonic control is usually realized in a centralized harmonic controller (see Fig. 3), which distributes the harmonic compensation reference signals to the distributed IFCs with communication links [133], [171]. Thus, the harmonic compensation efforts can be further optimized rather than simply determined by the IFCs power ratings. For example, in [93], modal analysis is used to provide priority factors for the IFCs in the AC microgrid considering the IFCs' power ratings and critical nodes of the system to compensate harmonics. This method provides a high-quality AC voltage at the lowest cost. The results of this example are shown in Fig. 24. In this simulation, the AC-coupled microgrid

TABLE 2. Summary of harmonics compensation in hybrid AC/DC microgrids using IFCs.

Harmonic Compensation in Hybrid AC/DC Microgrids by Interfacing Converters (IFCs)							
AC Harmonics Compensation						DC Ripple Mitigation	
Individual IFCs				Multiple IFCs Coordination			
Medium or Low Power IFCs			High Power IFCs				
(1) Current Control Method (CCM):	(2) Voltage Control Method (VCM):	(3) Hybrid Control Method (HCM):	(4) Feed Forward Method:	(5) Autonomous Harmonic Sharing:	(6) Supervisory Harmonic Sharing:	(7) Using DC-AC IFCs:	(8) Using DC-DC IFCs:
- Direct control of IFC's output current - Adjustable compensation - Not recommended for islanded mode - Better harmonic control dynamics than (2)	- Direct control of capacitor voltage -Adjustable compensation - Can operate at both grid-connected and islanded condition	- Parallel control of both output current and capacitor voltage -Adjustable compensation - Can operate at both grid-connected and islanded modes - Similar dynamics to (1)	-Harmonic control signal is directly fed into modulation index -Adjustable compensation - Good dynamics in low switching frequency converters - Less robust than (1)-(3) as no feedback loop for harmonic control	-Communication not required - Sharing errors cannot be corrected	- Communication required - Autonomous harmonic sharing capability can be added to increase robustness - Coordination can be made to optimize the compensation performance	- No need to add extra circuits - Affect AC-side control system - Centralized compensation	- Dedicated DC ripple mitigation devices can lead to extra cost - No impact on AC side - Distributed compensation

with 11 nodes, which contains the IFCs in each node, is used. As expected, when the harmonic compensation efforts are coordinated by given different priorities, the THD is lower than the case when all the IFCs do the harmonic compensation with the same priority.

In Table 2, a summary of all discussed control strategies of IFCs for harmonic compensation in Section V and their advantages and shortcoming are summarized.

VI. SUMMARY AND CONCLUSIONS

This paper has reviewed power quality control of the smart hybrid AC/DC microgrids with comprehensive discussions on the real-world microgrids' power quality issues. The primary and supervisory control strategies of the smart interfacing power converters in the hybrid AC/DC microgrids have been thoroughly reviewed to integrate power quality compensation. Also, coordination of the multiple interfacing power converters for the power quality control has been addressed in detail. In this paper, implementation examples of representative control schemes have been presented to better illustrate the power quality compensation by using the interfacing power converters.

Considering new policies and markets, revisions of standards and grid codes, modifications of communication protocols, and evolving control technique, the ancillary function of smart interfacing power converters to control the power quality are promoting. They can also further improve the system cost-effectiveness and are more effective than centralized compensation due to the distributed loads. It is expected that in the future, the IFCs in both DC and AC subgrids (single-phase and three-phase IFCs) will collaborate to compensate the unbalance condition in three-phase AC subgrid as well as control the voltage variations in DC subgrid at the same time. Also, it is expected that the IFCs will help to compensate the voltage harmonics instead of simply rejecting current harmonics and producing sinusoidal currents. Meanwhile, a new sampling scheme and corresponding multi-rate control will make it possible to compensate harmonic with low switching converters. Thus, the harmonic control will be widely performed by converters with different power rating, switching frequency, and filter design. The coordination of harmonic sharing and system level optimization will be also a promising idea.

REFERENCES

[1] F. Blaabjerg, "Driving power electronics into the future—Quo vadis," *IEEE Power Electron. Mag., Powering Past, Energizing Future*, pp. 9–11, Mar. 2018.

[2] R. Edge, B. York, and N. Enbar, "Rolling out smart inverters: Assessing 1245 utility strategies and approaches," Power Del. Utilization, Technical Results, Tech. Rep. 3002007047, Nov. 2015, p. 16.

[3] *Common Functions for Smart Inverters*, 4th ed., EPRI, Palo Alto, CA, USA: 2016.

[4] Pinnacle West Capital Corporation Annual Report. (2014). *Follow a Leader*. [Online]. Available: http://s22.q4cdn.com/464697698/files/doc_financials/annual/2014/2014AnnualReport_PinnacleWest.pdf

[5] *IEEE Standard for Interconnection and Interoperability of Distributed Energy Resources With Associated Electric Power Systems Interfaces*, IEEE Standard 1547-2018 (Revision of IEEE Standard 1547-2003), pp. 1–138, Apr. 2018.

[6] California Energy Commission. *Rule 21 Smart Inverter Working Group Technical Reference Materials*. Accessed: Mar. 11, 2014. [Online]. Available: http://www.energy.ca.gov/electricity_analysis/rule21/

[7] D. Salles, C. Jiang, W. Xu, W. Freitas, and H. E. Mazin, "Assessing the collective harmonic impact of modern residential loads—Part I: Methodology," *IEEE Trans. Power Del.*, vol. 27, no. 4, pp. 1937–1946, Oct. 2012.

[8] F. Nejabatkhah and Y. W. Li, "Overview of power management strategies of hybrid AC/DC microgrid," *IEEE Trans. Power Electron.*, vol. 30, no. 12, pp. 7072–7089, Dec. 2015.

[9] *DC Power for Data Centers*, Electr. Power Res. Inst., Palo Alto, CA, USA, Nov. 2010

[10] S. Rajagopalan, B. Fortenbery, and D. Symanski, "Power quality disturbances within DC data centers," in *Proc. Intelec*, Orlando, FL, USA, Jun. 2010, pp. 1–7.

[11] *Standardization Landscape for the Energy Management and Environmental Viability of Data Centres*, 4th ed., CEN/CLC/ETSI Joint Collaboration Rep., Brussels, Belgium, 2017.

[12] M. Ton, B. Fortenbery, and W. Tschudi, "DC power for improved data center efficiency," Lawrence Berkeley Nat. Lab., Berkeley, CA, USA, Joint Collaboration Rep., Mar. 2008. [Online]. Available: http://www.chip2grid.com/docs/DCDemoFinalReport.pdf

[13] M. Yilmaz and P. T. Krein, "Review of battery charger topologies, charging power levels, and infrastructure for plug-in electric and hybrid vehicles," *IEEE Trans. Power Electron.*, vol. 28, no. 5, pp. 2151–2169, May 2013.

[14] L. Tan, B. Wu, V. Yaramasu, S. Rivera, and X. Guo, "Effective voltage balance control for bipolar-DC-bus-fed EV charging station with three-level DC–DC fast charger," *IEEE Trans. Ind. Electron.*, vol. 63, no. 7, pp. 4031–4041, Jul. 2016.

[15] S. Bai and S. M. Lukic, "Unified active filter and energy storage system for an MW electric vehicle charging station," *IEEE Trans. Power Electron.*, vol. 28, no. 12, pp. 5793–5803, Dec. 2013.

[16] S. Rivera, B. Wu, S. Kouro, V. Yaramasu, and J. Wang, "Electric vehicle charging station using a neutral point clamped converter with bipolar DC bus," *IEEE Trans. Ind. Electron.*, vol. 62, no. 4, pp. 1999–2009, Apr. 2015.

[17] C. Russell and S. Wang, "DQ-frame modeling of an active power filter integrated with a grid-connected, multifunctional electric vehicle charging station," *IEEE Trans. Power Electron.*, vol. 28, no. 12, pp. 5702–5716, Dec. 2013.

[18] M. Vasiladiotis and A. Rufer, "A modular multiport power electronic transformer with integrated split battery energy storage for versatile ultrafast EV charging stations," *IEEE Trans. Ind. Electron.*, vol. 62, no. 5, pp. 3213–3222, May 2015.

[19] S. M. M. Gazafrudi, A. T. Langerudy, E. F. Fuchs, and K. Al-Haddad, "Power quality issues in railway electrification: A comprehensive perspective," *IEEE Trans. Ind. Electron.*, vol. 62, no. 5, pp. 3081–3090, May 2015.

[20] F. Ma, A. Luo, X. Xu, H. Xiao, C. Wu, and W. Wang, "A simplified power conditioner based on half-bridge converter for high-speed railway system," *IEEE Trans. Ind. Electron.*, vol. 60, no. 2, pp. 728–738, Feb. 2013.

[21] ABB. *FACTS Solutions for Railways*. Accessed: Jan. 18, 2019. [Online]. Available: https://new.abb.com/facts/solutions-for-railways

[22] *Power Quality in Internet Data Centers*, Electr. Power Res. Inst., Palo Altok, CA, USA, Nov. 2007.

[23] P. Matwijec and E. Spears, "Mitigating data center harmonics," Eaton Power Qual., Pondicherry, India, White Paper WP156001EN, Jan. 2014.

[24] M. Glinkowski *et al.*, "Data center power system harmonics: An overview of effects on data center efficiency and reliability," Green Grid Assoc., 2014.

[25] H. Zubi and S. Khalifa, "Power quality investigation of a typical telecom data centre electrical network," in *Proc. 4th Int. Conf. Control Eng. Inf. Technol. (CEIT)*, Hammamet, Tunisia, Dec. 2016, pp. 1–7.

[26] C.-L. Su, J.-T. Yu, H.-M. Chin, and C.-L. Kuo, "Evaluation of power-quality field measurements of an electric bus charging station using remote monitoring systems," in *Proc. 10th Int. Conf. Compat., Power Electron. Power Eng. (CPE-POWERENG)*, Bydgoszcz, Poland, Jun./Jul. 2016, pp. 58–63.

[27] Q. Li, S. Tao, X. Xiao, and J. Wen, "Monitoring and analysis of power quality in electric vehicle charging stations," in *Proc. 1st Int. Future Energy Electron. Conf. (IFEEC)*, Tainan, Taiwan, Nov. 2013, pp. 277–282.

[28] K. Clement-Nyns, E. Haesen, and J. Driesen, "The impact of charging plug-in hybrid electric vehicles on a residential distribution grid," *IEEE Trans. Power Syst.*, vol. 25, no. 1, pp. 371–380, Feb. 2010.

[29] J. M. Sexauer, K. D. McBee, and K. A. Bloch, "Applications of probability model to analyze the effects of electric vehicle chargers on distribution transformers," *IEEE Trans. Power Syst.*, vol. 28, no. 2, pp. 847–854, May 2013.

[30] L. Kutt, E. Saarijärvi, M. Lehtonen, H. Mõlder, and J. Niitsoo, "A review of the harmonic and unbalance effects in electrical distribution networks due to EV charging," in *Proc. IEEE Int. Conf. Environ. Elect. Eng.*, May 2013, pp. 556–561.

[31] C. Wenge, T. Winkler, M. Stötzer, and P. Komarnicki, "Power quality measurements of electric vehicles in the low voltage power grid," in *Proc. 11th Int. Conf. Elect. Power Quality Utilisation*, Oct. 2011, pp. 1–5.

[32] A. Javadi, A. Ndtoungou, H. F. Blanchette, and K. Al-Haddad, "Power quality device for future household systems with fast electric vehicle charging station," in *Proc. IEEE Vehicle Power Propuls. Conf. (VPPC)*, Montreal, QC, Canada, Oct. 2015, pp. 1–6.

[33] A. Ul-Haq, C. Buccella, C. Cecati, and H. A. Khalid, "Smart charging infrastructure for electric vehicles," in *Proc. Int. Conf. Clean Elect. Power (ICCEP)*, Alghero, Italy, Jun. 2013, pp. 163–169.

[34] M. Falahi, H.-M. Chou, M. Ehsani, L. Xie, and K. L. Butler-Purry, "Potential power quality benefits of electric vehicles," *IEEE Trans. Sustain. Energy*, vol. 4, no. 4, pp. 1016–1023, Oct. 2013.

[35] S.-L. Chen, R. J. Li, and P.-H. Hsi, "Traction system unbalance problem-analysis methodologies," *IEEE Trans. Power Del.*, vol. 19, no. 4, pp. 1877–1883, Oct. 2004.

[36] A. von Jouanne and B. Banerjee, "Assessment of voltage unbalance," *IEEE Trans. Power Del.*, vol. 16, no. 4, pp. 782–790, Oct. 2001.

[37] M. Z. El-Sadek, "Static VAr compensation for phase balancing and power factor improvement of single phase train loads," *Electr. Mach. Power Syst.*, vol. 26, no. 4, pp. 347–361, 1998.

[38] P.-C. Tan, R. E. Morrison, and D. G. Holmes, "Voltage form factor control and reactive power compensation in a 25-kV electrified railway system using a shunt active filter based on voltage detection," *IEEE Trans. Ind. Appl.*, vol. 39, no. 2, pp. 575–581, Mar. 2003.

[39] S. Senini and P. J. Wolfs, "Hybrid active filter for harmonically unbalanced three phase three wire railway traction loads," *IEEE Trans. Power Electron.*, vol. 15, no. 4, pp. 702–710, Jul. 2000.

[40] Z. Sun, X. Jiang, D. Zhu, and G. Zhang, "A novel active power quality compensator topology for electrified railway," *IEEE Trans. Power Electron.*, vol. 19, no. 4, pp. 1036–1042, Jul. 2004.

[41] Y. Li and F. Nejabatkhah, "Overview of control, integration and energy management of microgrids," *J. Mod. Power Syst. Clean Energy*, vol. 2, no. 3, pp. 212–222, Sep. 2014.

[42] A. Yazdani and R. Iravani, *Voltage-Sourced Converters in Power Systems: Modeling, Control, and Applications*. New York, NY, USA: Wiley, 2010.

[43] P. C. Loh, D. Li, Y. K. Chai, and F. Blaabjerg, "Autonomous operation of hybrid microgrid with ac and dc subgrids," *IEEE Trans. Power Electron.*, vol. 28, no. 5, pp. 2214–2223, May 2013.

[44] P. C. Loh, D. Li, Y. K. Chai, and F. Blaabjerg, "Autonomous control of interlinking converter with energy storage in hybrid AC–DC microgrid," *IEEE Trans. Ind. Appl.*, vol. 49, no. 3, pp. 1374–1383, May 2013.

[45] Q.-C. Zhong and G. Weiss, "Synchronverters: Inverters that mimic synchronous generators," *IEEE Trans. Ind. Electron.*, vol. 58, no. 4, pp. 1259–1267, Apr. 2011.

[46] Q.-C. Zhong, P.-L. Nguyen, Z. Ma, and W. Sheng, "Self-synchronized synchronverters: Inverters without a dedicated synchronization unit," *IEEE Trans. Power Electron.*, vol. 29, no. 2, pp. 617–630, Feb. 2014.

[47] E. Unamuno and J. A. Barrena, "Hybrid ac/dc microgrids—Part II: Review and classification of control strategies," *Renew. Sustain. Energy Rev.*, vol. 52, pp. 1123–1134, Dec. 2015.

[48] *American National Standard for Electric Power Systems and Equipment-Voltage Ratings (60 Hertz)*, Nat. Elect. Manufacturers Assoc., Washington, DC, USA, 1996.

[49] *IEEE Recommended Practice for Monitoring Electric Power Quality*, IEEE Standard 1159-2009 (Revision of IEEE Standard 1159-1995), Jun. 2009, p. c1-81.

[50] T.-L. Lee, S.-H. Hu, and Y.-H. Chan, "D-STATCOM with positive-sequence admittance and negative-sequence conductance to mitigate voltage fluctuations in high-level penetration of distributed-generation systems," *IEEE Trans. Ind. Electron.*, vol. 60, no. 4, pp. 1417–1428, Apr. 2013.

[51] M. Savaghebi, A. Jalilian, J. C. Vasquez, and J. M. Guerrero, "Autonomous voltage unbalance compensation in an islanded droop-controlled microgrid," *IEEE Trans. Ind. Electron.*, vol. 60, no. 4, pp. 1390–1402, Apr. 2013.

[52] D. Graovac, V. Katic, and A. Rufer, "Power quality problems compensation with universal power quality conditioning system," *IEEE Trans. Power Del.*, vol. 22, no. 2, pp. 968–976, Apr. 2007.

[53] F. Barrero, S. Martinez, F. Yeves, F. Mur, and P. M. Martinez, "Universal and reconfigurable to UPS active power filter for line conditioning," *IEEE Trans. Power Del.*, vol. 18, no. 1, pp. 283–290, Jan. 2003.

[54] S. George and V. Agarwal, "A DSP based optimal algorithm for shunt active filter under nonsinusoidal supply and unbalanced load conditions," *IEEE Trans. Power Electron.*, vol. 22, no. 2, pp. 593–601, Mar. 2007.

[55] B. Singh and J. Solanki, "An implementation of an adaptive control algorithm for a three-phase shunt active filter," *IEEE Trans. Ind. Electron.*, vol. 56, no. 8, pp. 2811–2820, Aug. 2009.

[56] F. Wang, J. L. Duarte, and M. A. M. Hendrix, "Grid-interfacing converter systems with enhanced voltage quality for microgrid application—Concept and implementation," *IEEE Trans. Power Electron.*, vol. 26, no. 12, pp. 3501–3513, Dec. 2011.

[57] J. M. Guerrero, P. C. Loh, T.-L. Lee, and M. Chandorkar, "Advanced control architectures for intelligent microgrids—Part II: Power quality, energy storage, and AC/DC microgrids," *IEEE Trans. Ind. Electron.*, vol. 60, no. 4, pp. 1263–1270, Apr. 2013.

[58] M. Castilla, J. Miret, A. Camacho, J. Matas, and L. G. de Vicuña, "Voltage support control strategies for static synchronous compensators under unbalanced voltage sags," *IEEE Trans. Ind. Electron.*, vol. 61, no. 2, pp. 808–820, Feb. 2014.

[59] K. Yunus, H. Z. De La Parra, and M. Reza, "Distribution grid impact of Plug-In Electric Vehicles charging at fast charging stations using stochastic charging model," in *Proc. 14th Eur. Conf. Power Electron. Appl. (EPE)*, Aug./Sep. 2011, pp. 1–11.

[60] P. Juanuwattanakul, M. A. S. Masoum, and S. Hajforoosh, "Application of SVC and single-phase shunt capacitor to improve voltage profiles and reduce losses of unbalanced multiphase smart grid with PEV charging stations," in *Proc. 22nd Australas. Universities Power Eng. Conf. (AUPEC)*, Bali, Indonesia, Sep. 2012, pp. 1–6.

[61] A. Camacho, M. Castilla, J. Miret, A. Borrell, and L. G. de Vicuña, "Active and reactive power strategies with peak current limitation for distributed generation inverters during unbalanced grid faults," *IEEE Trans. Ind. Electron.*, vol. 62, no. 3, pp. 1515–1525, Mar. 2015.

[62] J. Miret, M. Castilla, A. Camacho, L. G. de Vicuña, and J. Matas, "Control scheme for photovoltaic three-phase inverters to minimize peak currents during unbalanced grid-voltage sags," *IEEE Trans. Power Electron.*, vol. 27, no. 10, pp. 4262–4271, Oct. 2012.

[63] C. T. Lee, C. W. Hsu, and P. T. Cheng, "A low-voltage ride-through technique for grid-connected converters of distributed energy resources," *IEEE Trans. Ind. Appl.*, vol. 47, no. 4, pp. 1821–1832, Jul. 2011.

[64] S. Alepuz *et al.*, "Control strategies based on symmetrical components for grid-connected converters under voltage dips," *IEEE Trans. Ind. Electron.*, vol. 56, no. 6, pp. 2162–2173, Jun. 2009.

[65] F. Nejabatkhah, Y. W. Li, and B. Wu, "Control strategies of three-phase distributed generation inverters for grid unbalanced voltage compensation," *IEEE Trans. Power Electron.*, vol. 31, no. 7, pp. 5228–5241, Jul. 2016.

[66] R. Teodorescu, M. Liserre, and P. Rodrıguez, *Grid Converters for Photovoltaic and Wind Power Systems*. New York, NY, USA: Wiley, 2011.

[67] A. Camacho, M. Castilla, J. Miret, J. C. Vasquez, and E. Alarcon-Gallo, "Flexible voltage support control for three-phase distributed generation inverters under grid fault," *IEEE Trans. Ind. Electron.*, vol. 60, no. 4, pp. 1429–1441, Apr. 2013.

[68] J. Miret, A. Camacho, M. Castilla, L. G. de Vicuña, and J. Matas, "Control scheme with voltage support capability for distributed generation inverters under voltage sags," *IEEE Trans. Power Electron.*, vol. 28, no. 11, pp. 5252–5262, Nov. 2013.

[69] P. Rodriguez, A. Luna, J. Hermoso, I. Etxeberria-Otadui, R. Teodorescu, and F. Blaabjerg, "Current control method for distributed generation power generation plants under grid fault conditions," in *Proc. IEEE 37th Annu. Conf. Ind. Electron. Soc. (IECON)*, Nov. 2011, pp. 1262–1269.

[70] J. Lu, F. Nejabatkhah, Y. Li, and B. Wu, "DG control strategies for grid voltage unbalance compensation," in *Proc. IEEE Energy Convers. Congr. Expo. (ECCE)*, Sep. 2014, pp. 2932–2939.
[71] S. Chaudhary, R. Teodorescu, P. Rodriguez, P. C. Kjaer, and A. M. Gole, "Negative sequence current control in wind power plants with VSC-HVDC connection," *IEEE Trans. Sustain. Energy*, vol. 3, no. 3, pp. 535–544, Jul. 2012.
[72] I. Etxeberria-Otadui, U. Viscarret, M. Caballero, A. Rufer, and S. Bacha, "New optimized PWM VSC control structures and strategies under unbalanced voltage transients," *IEEE Trans. Ind. Electron.*, vol. 54, no. 5, pp. 2902–2914, Oct. 2007.
[73] F. Wang, J. L. Duarte, and M. A. M. Hendrix, "Pliant active and reactive power control for grid-interactive converters under unbalanced voltage dips," *IEEE Trans. Power Electron.*, vol. 26, no. 5, pp. 1511–1521, May 2011.
[74] P. T. Cheng, C. A. Chen, T. L. Lee, and S. Y. Kuo, "A cooperative imbalance compensation method for distributed-generation interface converters," *IEEE Trans. Ind. Appl.*, vol. 45, no. 2, pp. 805–815, Mar. 2009.
[75] F. Wang, H. Mao, D. Xu, and Y. Ruan, "Negative-sequence admittance control scheme for distributed compensation of grid voltage unbalance," in *Proc. IEEE 13th Workshop Control Modeling Power Electron. (COMPEL)*, Jun. 2012, pp. 1–8.
[76] M. Hamzeh, H. Karimi, and H. Mokhtari, "A new control strategy for a multi-bus MV microgrid under unbalanced conditions," *IEEE Trans. Power Sys.*, vol. 27, no. 4, pp. 2225–2233, Nov. 2012.
[77] D. De and V. Ramanarayanan, "Decentralized parallel operation of inverters sharing unbalanced and nonlinear loads," *IEEE Trans. Power Electron.*, vol. 25, no. 12, pp. 3015–3025, Dec. 2010.
[78] M. Savaghebi, A. Jalilian, J. C. Vasquez, and J. M. Guerrero, "Secondary control scheme for voltage unbalance compensation in an islanded droop-controlled microgrid," *IEEE Trans. Smart Grid*, vol. 3, no. 2, pp. 797–808, Jun. 2012.
[79] F. Nejabatkhah, Y. W. Li, and K. Sun, "Parallel three-phase interfacing converters operation under unbalanced voltage in hybrid AC/DC microgrid," *IEEE Trans. Smart Grid*, vol. 9, no. 2, pp. 1310–1322, Mar. 2018.
[80] K. Sun, X. Wang, Y. W. Li, F. Nejabatkhah, Y. Mei, and X. Lu, "Parallel operation of bidirectional interfacing converters in a hybrid AC/DC microgrid under unbalanced grid voltage conditions," *IEEE Trans. Power Electron.*, vol. 32, no. 3, pp. 1872–1884, Mar. 2017.
[81] F. Nejabatkhah, Y. W. Li, K. Sun, and R. Zhang, "Active power oscillation cancelation with peak current sharing in parallel interfacing converters under unbalanced voltage," *IEEE Trans. Power Electron.*, vol. 33, no. 12, pp. 10200–10214, Dec. 2018.
[82] H. Akagi, E. Watanabe, and M. Aredes, *Instantaneous Power Theory and Applications to Power Conditioning*. Hoboken, NJ, USA: Wiley, 2007.
[83] F. Wang, J. L. Duarte, and M. A. M. Hendrix, "Design and analysis of active power control strategies for distributed generation inverters under unbalanced grid faults," *IET Gener., Transmiss. Distrib.*, vol. 4, no. 8, pp. 905–916, 2010.
[84] F. Nejabatkhah and Y. W. Li, "Flexible unbalanced compensation of three-phase distribution system using single-phase distributed generation inverters," *IEEE Trans. Smart Grid*, vol. 10, no. 2, pp. 1845–1857, Mar. 2019.
[85] M. Coppo, A. Raciti, R. Caldon, and R. Turri, "Exploiting inverter-interfaced DG for Voltage unbalance mitigation and ancillary services in distribution systems," in *Proc. IEEE 1st Int. Forum Res. Technol. Soc. Ind. Leveraging Better Tomorrow (RTSI)*, Turin, Italy, Sep. 2015, pp. 371–376.
[86] R. Caldon, M. Coppo, and R. Turri, "Coordinated voltage control in MV and LV distribution networks with inverter-interfaced users," in *Proc. IEEE Grenoble Conf.*, Grenoble, France, Jun. 2013, pp. 1–5.
[87] R. Caldon, M. Coppo, and R. Turri, "A network voltage control strategy for LV inverter interfaced users," in *Proc. 8th Medit. Conf. Power Gener., Transmiss., Distrib. Energy Convers. (MEDPOWER)*, Cagliari, Italy, 2012, pp. 1–5.
[88] J. Fernandez, S. Bacha, D. Riu, H. Turker, and M. Paupert, "Current unbalance reduction in three-phase systems using single phase PHEV chargers," in *Proc. IEEE Int. Conf. Ind. Technol. (ICIT)*, Cape Town, South Africa, Feb. 2013, pp. 1940–1945.
[89] R. Caldon, M. Coppo, and R. Turri, "Voltage unbalance compensation in LV networks with inverter interfaced distributed energy resources," in *Proc. IEEE Int. Energy Conf. Exhib. (ENERGYCON)*, Florence, Italy, Sep. 2012, pp. 527–532.
[90] R. Caldon, M. Coppo, M. Tessari, and R. Turri, "Use of single-phase inverter-interfaced DGs for power quality improvement in LV networks," in *Proc. 47th Int. Universities Power Eng. Conf. (UPEC)*, London, U.K., Sep. 2012, pp. 1–5.
[91] *Test Feeder Cases*. Accessed: 1992. [Online]. Available: http://sites.ieee.org/pes-testfeeders/resources/
[92] X. Wang, F. Blaabjerg, and Z. Chen, "Autonomous control of inverter-interfaced distributed generation units for harmonic current filtering and resonance damping in an islanded microgrid," *IEEE Trans. Ind. Appl.*, vol. 50, no. 1, pp. 452–461, Jan./Feb. 2014.
[93] M. S. Munir, Y. W. Li, and H. Tian, "Improved residential distribution system harmonic compensation scheme using power electronics interfaced DGs," *IEEE Trans. Smart Grid*, vol. 7, no. 3, pp. 1191–1203, May 2016.
[94] J.-H. Seo, T.-K. Chung, C.-G. Lee, S.-Y. Jung, and H.-K. Jung, "Harmonic iron loss analysis of electrical machines for high-speed operation considering driving condition," *IEEE Trans. Magn.*, vol. 45, no. 10, pp. 4656–4659, Oct. 2009.
[95] X. Yuan, W. Merk, H. Stemmler, and J. Allmeling, "Stationary-frame generalized integrators for current control of active power filters with zero steady-state error for current harmonics of concern under unbalanced and distorted operating conditions," *IEEE Trans. Ind. Appl.*, vol. 38, no. 2, pp. 523–532, Mar./Apr. 2002.
[96] Z. Xin, P. Mattavelli, W. Yao, Y. Yang, F. Blaabjerg, and P. C. Loh, "Mitigation of grid-current distortion for LCL-filtered voltage-source inverter with inverter-current feedback control," *IEEE Trans. Power Electron.*, vol. 33, no. 7, pp. 6248–6261, Jul. 2017.
[97] D. De and V. Ramanarayanan, "A proportional + multiresonant controller for three-phase four-wire high-frequency link inverter," *IEEE Trans. Power Electron.*, vol. 25, no. 4, pp. 899–906, Apr. 2010.
[98] A. G. Yepes, F. D. Freijedo, O. Lopez, and J. Doval-Gandoy, "High-performance digital resonant controllers implemented with two integrators," *IEEE Trans. Power Electron.*, vol. 26, no. 2, pp. 563–576, Feb. 2011.
[99] A. G. Yepes, F. D. Freijedo, J. Doval-Gandoy, O. López, J. Malvar, and P. Fernandez-Comesaña, "Effects of discretization methods on the performance of resonant controllers," *IEEE Trans. Power Electron.*, vol. 25, no. 7, pp. 1692–1712, Jul. 2010.
[100] R. I. Bojoi, G. Griva, V. Bostan, M. Guerriero, F. Farina, and F. Profumo, "Current control strategy for power conditioners using sinusoidal signal integrators in synchronous reference frame," *IEEE Trans. Power Electron.*, vol. 20, no. 6, pp. 1402–1412, Nov. 2005.
[101] I. Etxeberria-Otadui, A. L. D. Heredia, H. Gaztanaga, S. Bacha, and M. R. Reyero, "A single synchronous frame hybrid (SSFH) multifrequency controller for power active filters," *IEEE Trans. Ind. Electron.*, vol. 53, no. 5, pp. 1640–1648, Oct. 2006.
[102] A. Kulkarni and V. John, "Mitigation of lower order harmonics in a grid-connected single-phase PV inverter," *IEEE Trans. Power Electron.*, vol. 28, no. 11, pp. 5024–5037, Nov. 2013.
[103] M. Castilla, J. Miret, J. Matas, L. Garcia de Vicuna, and J. M. Guerrero, "Control design guidelines for single-phase grid-connected photovoltaic inverters with damped resonant harmonic compensators," *IEEE Trans. Ind. Electron.*, vol. 56, no. 11, pp. 4492–4501, Nov. 2009.
[104] R. Costa-Castelló, R. Griñó, and E. Fossas, "Odd-harmonic digital repetitive control of a single-phase current active filter," *IEEE Trans. Power Electron.*, vol. 19, no. 4, pp. 1060–1068, Jul. 2004.
[105] G. Escobar, P. R. Martinez, J. Leyva-Ramos, and P. Mattavelli, "A negative feedback repetitive control scheme for harmonic compensation," *IEEE Trans. Ind. Electron.*, vol. 53, no. 4, pp. 1383–1386, Jun. 2006.
[106] K. Zhou, Y. Yang, F. Blaabjerg, and D. Wang, "Optimal selective harmonic control for power harmonics mitigation," *IEEE Trans. Ind. Electron.*, vol. 62, no. 2, pp. 1220–1230, Feb. 2015.
[107] P. Loh, Y. Tang, F. Blaabjerg, and P. Wang, "Mixed-frame and stationary-frame repetitive control schemes for compensating typical load and grid harmonics," *IET Trans. Power Electron.*, vol. 4, no. 2, pp. 218–226, 2011.
[108] G. Escobar, P. G. Hernandez-Briones, P. R. Martinez, M. Hernandez-Gomez, and R. E. Torres-Olguin, "A repetitive-based controller for the compensation of 6k 1 harmonic components," *IEEE Trans. Ind. Electron.*, vol. 55, no. 8, pp. 3150–3158, Aug. 2008.
[109] P. Mattavelli and F. P. Marafao, "Repetitive-based control for selective harmonic compensation in active power filters," *IEEE Trans. Ind. Electron.*, vol. 51, no. 5, pp. 1018–1024, Oct. 2004.

[110] Q. N. Trinh, P. Wang, T. Yi, and F. H. Choo, "Mitigation of DC and harmonic currents generated by voltage measurement errors and grid voltage distortions in transformerless grid-connected inverters," *IEEE Trans. Energy Convers.*, vol. 33, no. 2, pp. 801–813, Jun. 2018.

[111] C. Xie, X. Zhao, M. Savaghebi, L. Meng, J. M. Guerrero, and J. C. Vasquez, "Multirate fractional-order repetitive control of shunt active power filter suitable for microgrid applications," *IEEE J. Emerg. Sel. Topics Power Electron.*, vol. 5, no. 2, pp. 809–819, Jun. 2017.

[112] D. Chen, J. Zhang, and Z. Qian, "An improved repetitive control scheme for grid-connected inverter with frequency-adaptive capability," *IEEE Trans. Ind. Electron.*, vol. 60, no. 2, pp. 814–823, Feb. 2013.

[113] T. Hornik and Q.-C. Zhong, "H^{∞} repetitive voltage control of grid-connected inverters with a frequency adaptive mechanism," *IET Trans. Power Electron.*, vol. 3, no. 6, pp. 925–935, 2010.

[114] Y. Yang, K. Zhou, H. Wang, F. Blaabjerg, D. Wang, and B. Zhang, "Frequency adaptive selective harmonic control for grid-connected inverters," *IEEE Trans. Power Electron.*, vol. 30, no. 7, pp. 3912–3924, Jul. 2015.

[115] J. He, Y. W. Li, D. Xu, X. Liang, B. Liang, and C. Wang, "Deadbeat weighted average current control with corrective feed-forward compensation for microgrid converters with nonstandard LCL filter," *IEEE Trans. Power Electron.*, vol. 32, no. 4, pp. 2661–2674, Apr. 2017.

[116] S. Buso, T. Caldognetto, and D. I. Brandao, "Dead-beat current controller for voltage-source converters with improved large-signal response," *IEEE Trans. Ind. Appl.*, vol. 52, no. 2, pp. 1588–1596, Mar./Apr. 2016.

[117] Q. Zeng and L. Chang, "An advanced SVPWM-based predictive current controller for three-phase inverters in distributed generation systems," *IEEE Trans. Ind. Electron.*, vol. 55, no. 3, pp. 1235–1246, Mar. 2008.

[118] W. Jiang, X. Ding, Y. Ni, J. Wang, L. Wang, and W. Ma, "An improved deadbeat control for a three-phase three-line active power filter with current-tracking error compensation," *IEEE Trans. Power Electron*, vol. 33, no. 3, pp. 2061–2072, Mar. 2017.

[119] D. Martin and E. Santi, "Autotuning of digital deadbeat current controllers for grid-tie inverters using wide bandwidth impedance identification," *IEEE Trans. Ind. Appl.*, vol. 50, no. 1, pp. 441–451, Jan./Feb. 2014.

[120] G. H. Bode, P. C. Loh, M. J. Newman, and D. G. Holmes, "An improved robust predictive current regulation algorithm," *IEEE Trans. Ind. Appl.*, vol. 41, no. 6, pp. 1720–1733, Nov. 2005.

[121] K. H. Ahmed, A. M. Massoud, S. J. Finney, and B. W. Williams, "A modified stationary reference frame-based predictive current control with zero steady-state error for LCL coupled inverter-based distributed generation systems," *IEEE Trans. Ind. Electron.*, vol. 58, no. 4, pp. 1359–1370, Apr. 2011.

[122] C. Lascu, L. Asiminoaei, L. Boldea, and F. Blaabjerg, "Frequency response analysis of current controllers for selective harmonic compensation in active power filters," *IEEE Trans. Ind. Electron.*, vol. 56, no. 2, pp. 337–347, Feb. 2009.

[123] C. J. Gajanayake, D. M. Vilathgamuwa, P. C. Loh, R. Teodorescu, and F. Blaabjerg, "Z-source-inverter-based flexible distributed generation system solution for grid power quality improvement," *IEEE Trans. Energy Convers.*, vol. 24, no. 3, pp. 695–704, Sep. 2009.

[124] J. He, Y. W. Li, F. Blaabjerg, and X. Wang, "Active harmonic filtering using current-controlled, grid-connected DG units with closed-loop power control," *IEEE Trans. Power Electron.*, vol. 29, no. 2, pp. 642–653, Feb. 2014.

[125] Y. Yang, K. Zhou, and F. Blaabjerg, "Current harmonics from single-phase grid-connected inverters-examination and suppression," *IEEE J. Emerg. Sel. Topics Power Electron.*, vol. 4, no. 1, pp. 221–233, Mar. 2016.

[126] Q.-N. Trinh and H.-H. Lee, "An enhanced grid current compensator for grid-connected distributed generation under nonlinear loads and grid voltage distortions," *IEEE Trans. Ind. Electron.*, vol. 61, no. 12, pp. 6528–6537, Dec. 2014.

[127] Y. Jia, J. Zhao, and X. Fu, "Direct grid current control of LCL-filtered grid-connected inverter mitigating grid voltage disturbance," *IEEE Trans. Power Electron.*, vol. 29, no. 3, pp. 1532–1541, Mar. 2014.

[128] H. Akagi, "Control strategy and site selection of a shunt active filter for damping of harmonic propagation in power distribution systems," *IEEE Trans. Power Del.*, vol. 12, no. 2, pp. 354–363, Jan. 1997.

[129] J. He, Y. W. Li, and M. S. Munir, "A flexible harmonic control approach through voltage-controlled DG–Grid interfacing converters," *IEEE Trans. Ind. Electron.*, vol. 59, no. 1, pp. 444–455, Jan. 2012.

[130] M. Hamzeh, H. Karimi, and H. Mokhtari, "Harmonic and negative-sequence current control in an islanded multi-bus MV microgrid," *IEEE Trans. Smart Grid*, vol. 5, no. 1, pp. 167–176, Jan. 2014.

[131] P. Sreekumar and V. Khadkikar, "A new virtual harmonic impedance scheme for harmonic power sharing in an islanded microgrid," *IEEE Trans. Power Del.*, vol. 31, no. 3, pp. 936–945, Jun. 2016.

[132] Q. Liu, Y. Tao, X. Liu, Y. Deng, and X. He, "Voltage unbalance and harmonics compensation for islanded microgrid inverters," *IET Trans. Power Electron.*, vol. 7, no. 5, pp. 1055–1063, May 2014.

[133] M. Savaghebi, A. Jalilian, J. C. Vásquez, and J. M. Guerrero, "Secondary control for voltage quality enhancement in microgrids," *IEEE Trans. Smart Grid*, vol. 3, no. 4, pp. 1893–1902, Dec. 2012.

[134] W. Feng, K. Sun, Y. Guan, J. M. Guerrero, and X. Xiao, "Active power quality improvement strategy for grid-connected microgrid based on hierarchical control," *IEEE Trans. Smart Grid*, vol. 9, no. 4, pp. 3486–3495, Jul. 2018.

[135] J. Wang, C. Jin, and P. Wang, "A uniform control strategy for the interlinking converter in hierarchical controlled hybrid AC/DC microgrids," *IEEE Trans. Ind. Electron.*, vol. 65, no. 8, pp. 6188–6197, Aug. 2018.

[136] Q. Huang and K. Rajashekara, "A unified selective harmonic compensation strategy using DG-interfacing inverter in both grid-connected and islanded microgrid," in *Proc. IEEE Energy Convers. Congr. Expo. (ECCE)*, Cincinnati, OH, USA, Oct. 2017, pp. 1588–1593.

[137] F. Tang, J. M. Guerrero, J. C. Vasquez, D. Wu, and L. Meng, "Distributed active synchronization strategy for microgrid seamless reconnection to the grid under unbalance and harmonic distortion," *IEEE Trans. Smart Grid*, vol. 6, no. 6, pp. 2757–2769, Nov. 2015.

[138] A. Micallef, M. Apap, C. Spiteri-Staines, and J. M. Guerrero, "Mitigation of harmonics in grid-connected and islanded microgrids via virtual admittances and impedances," *IEEE Trans. Smart Grid*, vol. 8, no. 2, pp. 651–661, Mar. 2017.

[139] H.-P. Beck and R. Hesse, "Virtual synchronous machine," in *Proc. 9th Int. Conf. Elect. Power Quality Utilisation*, Barcelona, Spain, Oct. 2007, pp. 1–6.

[140] H. Bevrani, T. Ise, and Y. Miura, "Virtual synchronous generators: A survey and new perspectives," *Int. J. Electr. Power Energy Syst.*, vol. 54, pp. 244–254, Jan. 2014.

[141] S. D'Arco and J. A. Suul, "Equivalence of virtual synchronous machines and frequency-droops for converter-based MicroGrids," *IEEE Trans. Smart Grid*, vol. 5, no. 1, pp. 394–395, Jan. 2014.

[142] X. Chen, X. Ruan, D. Yang, W. Zhao, and L. Jia, "Injected grid current quality improvement for a voltage-controlled grid-connected inverter," *IEEE Trans. Power Electron.*, vol. 33, no. 2, pp. 1247–1258, Feb. 2018.

[143] H. Tian, X. Wen, and Y. W. Li, "A harmonic compensation approach for interlinking voltage source converters in hybrid AC-DC microgrids with low switching frequency," *CSEE J. Power Energy Syst.*, vol. 4, no. 1, pp. 39–48, Mar. 2018.

[144] J. He and Y. W. Li, "Hybrid voltage and current control approach for DG-grid interfacing converters with LCL filters," *IEEE Trans. Ind. Electron.*, vol. 60, no. 5, pp. 1797–1809, May 2013.

[145] X. Zhao *et al.*, "A voltage feedback based harmonic compensation strategy for current-controlled converters," *IEEE Trans. Ind. Appl.*, vol. 54, no. 3, pp. 2616–2627, May/Jun. 2017.

[146] X. Wang, X. Ruan, S. Liu, and C. K. Tse, "Full feedforward of grid voltage for grid-connected inverter with LCL filter to suppress current distortion due to grid voltage harmonics," *IEEE Trans. Power Electron.*, vol. 25, no. 12, pp. 3119–3127, Dec. 2010.

[147] D. Yang, X. Ruan, and H. Wu, "Impedance shaping of the grid-connected inverter with LCL filter to improve its adaptability to the weak grid condition," *IEEE Trans. Power Electron.*, vol. 29, no. 11, pp. 5795–5805, Nov. 2014.

[148] X. Wu, X. Li, X. Yuan, and Y. Geng, "Grid harmonics suppression scheme for LCL-type grid-connected inverters based on output admittance revision," *IEEE Trans. Sustain. Energy*, vol. 6, no. 2, pp. 411–421, Apr. 2015.

[149] J. Xu, S. Xie, Q. Qian, and B. Zhang, "Adaptive feedforward algorithm without grid impedance estimation for inverters to suppress grid current instabilities and harmonics due to grid impedance and grid voltage distortion," *IEEE Trans. Ind. Electron.*, vol. 64, no. 9, pp. 7574–7586, Sep. 2017.

[150] H. Tian, Y. W. Li, and P. Wang, "Hybrid AC/DC system harmonics control through grid interfacing converters with low switching frequency," *IEEE Trans. Ind. Electron.*, vol. 65, no. 3, pp. 2256–2267, Mar. 2018.

[151] H. M. Kojabadi, B. Yu, I. A. Gadoura, L. Chang, and M. Ghribi, "A novel DSP-based current-controlled PWM strategy for single phase grid connected inverters," *IEEE Trans. Power Electron.*, vol. 21, no. 4, pp. 985–993, Jul. 2006.
[152] D. Yang, X. Ruan, and H. Wu, "A real-time computation method with dual sampling mode to improve the current control performance of the LCL-type grid-connected inverter," *IEEE Trans. Ind. Electron.*, vol. 62, no. 7, pp. 4563–4572, Jul. 2015.
[153] X. Zhang, P. Chen, C. Yu, F. Li, H. T. Do, and R. Cao, "Study of a current control strategy based on multisampling for high-power grid-connected inverters with an LCL filter," *IEEE Trans. Power Electron.*, vol. 32, no. 7, pp. 5023–5034, Jul. 2017.
[154] D. Kumar, F. Zare, and A. Ghosh, "DC microgrid technology: System architectures, AC grid interfaces, grounding schemes, power quality, communication networks, applications, and standardizations aspects," *IEEE Access*, vol. 5, pp. 12230–12256, 2017.
[155] Y. Jiang and A. Ekstrom, "General analysis of harmonic transfer through converters," *IEEE Trans. Power Electron.*, vol. 12, no. 2, pp. 287–293, Mar. 1997.
[156] Y. Du, D. D. C. Lu, G. M. L. Chu, and W. Xiao, "Closed-form solution of time-varying model and its applications for output current harmonics in two-stage PV inverter," *IEEE Trans. Sustain. Energy*, vol. 6, no. 1, pp. 142–150, Jan. 2015.
[157] N. Femia, G. Petrone, G. Spagnuolo, and M. Vitelli, "Optimization of perturb and observe maximum power point tracking method," *IEEE Trans. Power Electron.*, vol. 20, no. 4, pp. 963–973, Jul. 2005.
[158] W. Xiao, N. Ozog, and W. G. Dunford, "Topology study of photovoltaic interface for maximum power point tracking," *IEEE Trans. Ind. Electron.*, vol. 54, no. 3, pp. 1696–1704, Jun. 2007.
[159] J. Riedel, D. G. Holmes, B. P. McGrath, and C. Teixeira, "Active suppression of selected dc bus harmonics for dual active bridge DC–DC converters," *IEEE Trans. Power Electron.*, vol. 32, no. 11, pp. 8857–8867, Nov. 2017.
[160] P. N. Enjeti and W. Shireen, "A new technique to reject DC-link voltage ripple for inverters operating on programmed PWM waveforms," *IEEE Trans. Power Electron.*, vol. 7, no. 1, pp. 171–180, Jan. 1992.
[161] P. Rodriguez, A. V. Timbus, R. Teodorescu, M. Liserre, and F. Blaabjerg, "Flexible active power control of distributed power generation systems during grid faults," *IEEE Trans. Ind. Electron.*, vol. 54, no. 5, pp. 2583–2592, Oct. 2007.
[162] V. Valouch, M. Bejvl, P. Šimek, and J. Škramlík, "Power control of grid-connected converters under unbalanced voltage conditions," *IEEE Trans. Ind. Electron.*, vol. 62, no. 7, pp. 4241–4248, Jul. 2015.
[163] S. Li, A. T. L. Lee, S. C. Tan, and S. Y. R. Hui, "Plug-and-play voltage ripple mitigator for DC links in hybrid AC–DC power grids with local bus-voltage control," *IEEE Trans. Ind. Electron*, vol. 65, no. 1, pp. 687–698, Jan. 2018.
[164] L. Cao, K. H. Loo, and Y. M. Lai, "Frequency-adaptive filtering of low-frequency harmonic current in fuel cell power conditioning systems," *IEEE Trans. Power Electron*, vol. 30, no. 4, pp. 1966–1978, Apr. 2015.
[165] U. Borup, F. Blaabjerg, and P. N. Enjeti, "Sharing of nonlinear load in parallel-connected three-phase converters," *IEEE Trans. Ind. Appl.*, vol. 37, no. 6, pp. 1817–1823, Nov./Dec. 2001.
[166] P. Jintakosonwit, H. Akagi, H. Fujita, and S. Ogasawara, "Implementation and performance of automatic gain adjustment in a shunt-active filter for harmonic damping throughout a power distribution system," *IEEE Trans. Power Electron.*, vol. 17, no. 3, pp. 438–447, May 2002.
[167] Q.-C. Zhong, "Harmonic droop controller to reduce the voltage harmonics of inverters," *IEEE Trans. Ind. Electron.*, vol. 60, no. 3, pp. 936–945, Mar. 2013.
[168] P. Sreekumar and V. Khadkikar, "Direct control of the inverter impedance to achieve controllable harmonic sharing in the islanded microgrid," *IEEE Trans. Ind. Electron.*, vol. 64, no. 1, pp. 827–837, Jan. 2017.
[169] H. Moussa, A. Shahin, J.-P. Martin, B. Nahid-Mobarakeh, S. Pierfederici, and N. Moubayed, "Harmonic power sharing with voltage distortion compensation of droop controlled islanded microgrids," *IEEE Trans. Smart Grid*, vol. 9, no. 5, pp. 5335–5347, Sep. 2018.
[170] J. Zhou, S. Kim, H. Zhang, Q. Sun, and R. Han, "Consensus-based distributed control for accurate reactive, harmonic, and imbalance power sharing in microgrids," *IEEE Trans. Smart Grid*, vol. 9, no. 4, pp. 2453–2467, Jul. 2016.
[171] J. He, Y. W. Li, and F. Blaabjerg, "An enhanced islanding microgrid reactive power, imbalance power, and harmonic power sharing scheme," *IEEE Trans. Power Electron.*, vol. 30, no. 6, pp. 3389–3401, Jun. 2015.

FARZAM NEJABATKHAH (S'09–M'17) received the B.Sc. and M.Sc. degrees (Hons.) from the University of Tabriz, Tabriz, Iran, in 2009 and 2011, respectively, and the Ph.D. degree from the University of Alberta, Edmonton, Canada, in 2017, all in electrical engineering. Since 2017, he has been a Postdoctoral Research Fellow with the University of Alberta.

His research interests include ac-dc microgrids, smart grids, power quality, renewable generations and energy storages, and power electronic converters.

YUN WEI LI (S'04–M'05–SM'11) received the B.Sc. degree in electrical engineering from Tianjin University, Tianjin, China, in 2002, and the Ph.D. degree from Nanyang Technological University, Singapore, in 2006.

In 2005, he was a Visiting Scholar with Aalborg University, Denmark. From 2006 to 2007, he was a Postdoctoral Research Fellow with Ryerson University, Canada. In 2007, he was also with Rockwell Automation Canada before he joined the University of Alberta, Canada, in 2007. Since 2007, he has been with the University of Alberta, where he is currently a Professor. His research interests include distributed generation, microgrid, renewable energy, high power converters, and electric motor drives.

Dr. Li was a recipient of the Richard M. Bass Outstanding Young Power Electronics Engineer Award from IEEE Power Electronics Society, in 2013, and the Second Prize Paper Award of IEEE TRANSACTIONS ON POWER ELECTRONICS, in 2014. He was an Associate Editor of the IEEE TRANSACTIONS ON POWER ELECTRONICS, the IEEE TRANSACTIONS ON INDUSTRIAL ELECTRONICS, the IEEE TRANSACTIONS ON SMART GRID, and the IEEE JOURNAL OF EMERGING AND SELECTED TOPICS IN POWER ELECTRONICS. He serves as an Editor-in-Chief for the IEEE TRANSACTIONS ON POWER ELECTRONICS LETTERS.

HAO TIAN (S'12) received the B.Sc. and M.Eng. degrees in electrical engineering from Shandong University, Jinan, China, in 2011 and 2014, respectively. He is currently pursuing the Ph.D. degree with the University of Alberta, Edmonton, Canada.

His research interests include high power converters and power quality, and multilevel converters.